# The Partial Element Equivalent Circuit Method for EMI, EMC and SI Analysis

Giulio Antonini

*EMC Laboratory*
Dipartimento di Ingegneria Elettrica e dell'Informazione
Università degli Studi di L'Aquila
Poggio di Roio, 67040 AQ, Italy

## I. Introduction

The rapid growth of electrical modeling and analysis of electric and electronic systems is due to the increasing importance of the passive parasitic elements which are cause of interferences or may act as sources for electromagnetic compatibility and signal integrity problems. The electromagnetic nature of such effects along with the geometric complexity of electronic systems call for efficient electromagnetic methodologies and computer-aided design tools which allow a full-wave analysis of 3-D structures characterized by inhomogeneous materials and complex geometries.

The three most popular computational methods which are usually adopted in computational electromagnetics (CEM) are the finite element method (FEM) [1], the finite difference time domain (FDTD) [2]–[4] technique, and the method of moments (MoM) [5]. It is known that the first two approaches are essentially based on the partial differential equation (PDE) form of Maxwell's equations and result into powerful techniques that have been widely used for a variety of EM problems. The Method of Moments is based on an integral formulation of Maxwell's equations. Among all the different integral equation (IE) based techniques this tutorial focuses on the Partial Element Equivalent Circuit (PEEC) method. Stemming from the pioneering works by Ruehli [6]- [8], in this tutorial paper the PEEC method is revised with the aim to provide the reader with a step-by-step procedure to develop its own PEEC solver.

The main difference of PEEC method with other integral equation based techniques resides in the fact that it provides a circuit interpretation of the electric field integral equation [9] in terms of partial elements, namely resistances, partial inductances and coefficients of potential. Thus, the resulting equivalent circuit can be studied by means of Spice-like circuit solvers [10] in both time and frequency domain. Furthermore, once the PEEC model for an electromagnetic system has been developed, a systematic procedure can be used to reduce its complexity, taking into account the electrical size of the structure under analysis. For example, if the characteristic time of the excitation (i.e. the rise time of a pulsed excitation pr the period of a time-harmonic excitation) is such that useful wavelengths are much larger than the spatial extent of the system, all retardation effects can be neglected.

Integral equation (IE) methods are very effective for electromagnetic modeling for electromagnetic interference (EMI) and electromagnetic compatibility (EMC) purposes. The first step of any integral equation-based method is the development of an integral formulation of Maxwell's equation. The most popular integral equation is the electric field integral equation which is obtained by enforcing the electric field at a point in the structure as the superposition of fields due to all electric currents and charges in the system [9], [11].

Compared with differential equation (DE) based methods, the matrices resulting from IE based techniques solutions are smaller in size and dense. The reason for the reduced size is that the unknowns are represented by the electric currents flowing through the volumes of conductors dielectrics and charges on their surfaces; the reason for the density of matrices arising from IE solutions is that each element describes the electromagnetic interaction (electric and magnetic) between two discrete currents or charges in the structure.

The paper is organized as follows: Section II presents the basic derivation of the PEEC method starting from the volume electric field integral equation (EFIE); the synthesis of the PEEC equivalent circuit is revised in Section III and the computation of the partial elements in Section IV; the extension to dielectrics is described in Section V; a brief discussion of frequency and time domain solvers is presented in Section VI; Section VII reports numerical examples in EMC, EMI and SI areas; finally, Section VIII draws the conclusions. It is not in the scope of this article to discuss advanced PEEC modeling for which, the interested reader can refer to the referenced papers.

## II. PEEC Integral Formulation of Maxwell's Equations

Maxwell differential equation in time domain are [9]:

$$\nabla \times \boldsymbol{H}(\boldsymbol{r},t) = \frac{\partial \boldsymbol{D}(\boldsymbol{r},t)}{\partial t} + \boldsymbol{J}(\boldsymbol{r},t) \tag{1a}$$

$$\nabla \times \boldsymbol{E}(\boldsymbol{r},t) = -\frac{\partial \boldsymbol{B}(\boldsymbol{r},t)}{\partial t} \tag{1b}$$

$$\nabla \cdot \boldsymbol{B}(\boldsymbol{r},t) = 0 \tag{1c}$$

$$\nabla \cdot \boldsymbol{D}(\boldsymbol{r},t) = \varrho(\boldsymbol{r},t) \tag{1d}$$

where $\varrho(\boldsymbol{r},t)$ is the charge density and $\boldsymbol{J}(\boldsymbol{r},t)$ is the current density; the fields $\boldsymbol{H}, \boldsymbol{B}, \boldsymbol{E}$ and $\boldsymbol{D}$ satisfy the following constitutive relations:

$$\boldsymbol{B}(\boldsymbol{r},t) = \mu \boldsymbol{H}(\boldsymbol{r},t) \tag{2a}$$

$$\boldsymbol{D}(\boldsymbol{r},t) = \varepsilon \boldsymbol{E}(\boldsymbol{r},t) \tag{2b}$$

It is useful to express fields in terms of potential. From the divergenceless property (1c) of $\boldsymbol{B}$, we define the magnetic vector potential such that:

$$\boldsymbol{B}(\boldsymbol{r},t) = \nabla \times \boldsymbol{A}(\boldsymbol{r},t) \tag{3}$$

Substituting (3) into (1b) we obtain:

$$\nabla \times \left( \boldsymbol{E}(\boldsymbol{r},t) + \frac{\partial \boldsymbol{A}(\boldsymbol{r},t)}{\partial t} \right) = \boldsymbol{0} \tag{4}$$

The previous equation allows to define the electric scalar potential $\boldsymbol{\Phi}(\boldsymbol{r},t)$ such that:

$$\boldsymbol{E}(\boldsymbol{r},t) + \frac{\partial \boldsymbol{A}(\boldsymbol{r},t)}{\partial t} = -\nabla \Phi(\boldsymbol{r},t) \tag{5}$$

Such equation relates the electric field $\boldsymbol{E}$ with the potentials $\boldsymbol{A}$ and $\Phi$. The next step is to express such potentials $\boldsymbol{A}$ and $\Phi$ in terms of $\boldsymbol{J}$ and $\varrho$ respectively. To this aim we substitute (3) and (5) into (1a) we obtain

$$\nabla \times \nabla \times \boldsymbol{A}(\boldsymbol{r},t) = \mu\varepsilon \frac{\partial}{\partial t} \left( -\frac{\partial \boldsymbol{A}(\boldsymbol{r},t)}{\partial t} - \nabla \Phi(\boldsymbol{r},t) \right) - \mu \boldsymbol{J}(\boldsymbol{r},t) \tag{6}$$

Using the Laplacian identity

$$\nabla \times \nabla \times \boldsymbol{A}(\boldsymbol{r},t) = \nabla \left( \nabla \cdot \boldsymbol{A}(\boldsymbol{r},t) \right) - \nabla^2 \boldsymbol{A}(\boldsymbol{r},t) \tag{7}$$

and enforcing the Lorenz gauge

$$\nabla \cdot \boldsymbol{A}(\boldsymbol{r},t) = -\mu\varepsilon \frac{\partial \Phi(\boldsymbol{r},t)}{\partial t} \tag{8}$$

we finally obtain the Helmholtz equation for the magnetic vector potential:

$$\nabla^2 \boldsymbol{A}(\boldsymbol{r},t) - \mu\varepsilon \frac{\partial \boldsymbol{A}(\boldsymbol{r},t)}{\partial t^2} = -\mu \boldsymbol{J}(\boldsymbol{r},t) \tag{9}$$

Following the same steps it is possible to express the potential $\Phi(\boldsymbol{r},t)$ in terms of the charge density leading to the Helmholtz equation for the electric scalar potential

$$\nabla^2 \Phi(\boldsymbol{r},t) - \mu\varepsilon \frac{\partial \Phi(\boldsymbol{r},t)}{\partial t^2} = -\frac{\varrho(\boldsymbol{r},t)}{\varepsilon} \tag{10}$$

In an homogenous medium equation (9) has a closed-form solution for the magnetic vector potential $\boldsymbol{A}(\boldsymbol{r},t)$ due to a current $\boldsymbol{J}(\boldsymbol{r},t)$ in the volume $V'$; it is:

$$\boldsymbol{A}(\boldsymbol{r},t) = \frac{\mu}{4\pi}\int_{V'}\frac{\boldsymbol{J}(\boldsymbol{r}',t')}{|\boldsymbol{r}-\boldsymbol{r}'|}dV' \tag{11}$$

In an homogenous medium also equation (10) has a closed-form solution for the electric scalar potential $\Phi(\boldsymbol{r},t)$ due to the charge distribution $\varrho(\boldsymbol{r}',t)$; taking into account that the charge resides on the exterior surface of conductors, the solution of (10) in an homogenous medium is:

$$\Phi(\boldsymbol{r},t) = \frac{1}{4\pi\varepsilon}\int_{S'}\frac{\varrho(\boldsymbol{r}',t')}{|\boldsymbol{r}-\boldsymbol{r}'|}dS' \tag{12}$$

In equations (11) and (12) $t'$ denotes the time at which the current and charge distributions, $\boldsymbol{J}$ and $\varrho$, act as sources of $\boldsymbol{A}$ and $\Phi$ respectively; it is different from $t$ because of the finite value of the speed of light in the background homogenous medium, $c=1/\sqrt{\mu\varepsilon}$. it means that they can be related by:

$$t = t' - |\boldsymbol{r}-\boldsymbol{r}'|/c \tag{13}$$

In deriving relations (11) and (12) all the Maxwell's equations (1a-1d) have been used along with the Lorenz gauge (8). So far equation (5) for the electric field has not been used yet.

In a conductor the following constitutive relation holds:

$$\boldsymbol{E}(\boldsymbol{r},t) = \frac{\boldsymbol{J}(\boldsymbol{r},t)}{\sigma} \tag{14}$$

where $\sigma$ is the conductor conductivity. Substituting equation (14) into the electric field equation (5) and taking into account that an external electric field $\boldsymbol{E}_0(\boldsymbol{r},t)$ can be impressed at point $\boldsymbol{r}$ at time $t$, we obtain the electric field integral equation (EFIE)

$$\boldsymbol{E}_0(\boldsymbol{r},t) = \frac{\boldsymbol{J}(\boldsymbol{r},t)}{\sigma} + \frac{\partial}{\partial t}\frac{\mu}{4\pi}\int_{V'}\frac{\boldsymbol{J}(\boldsymbol{r}',t')}{|\boldsymbol{r}-\boldsymbol{r}'|}dV' + \nabla\Phi(\boldsymbol{r},t) \tag{15}$$

which holds at any point in a conductor and where the electric scalar potential is related to the charge distribution by equation (10), here repeated for clarity:

$$\Phi(\boldsymbol{r},t) = \frac{1}{4\pi\varepsilon}\int_{S'}\frac{\varrho(\boldsymbol{r}',t')}{|\boldsymbol{r}-\boldsymbol{r}'|}dS' \tag{16}$$

To ensure the conservation of charge the continuity must be enforced:

$$\nabla\cdot\boldsymbol{J}(\boldsymbol{r},t) = -\frac{\partial\varrho(\boldsymbol{r},t)}{\partial t} \tag{17}$$

As we have assumed that the charge is located only on the surface of conductors, in the interior of conductors equation (17) becomes:

$$\nabla\cdot\boldsymbol{J}(\boldsymbol{r},t) = 0 \tag{18}$$

while on the surface of conductors, using the surface divergence, we have:

$$\hat{\boldsymbol{n}}\cdot\boldsymbol{J}(\boldsymbol{r},t) = \frac{\partial\varrho(\boldsymbol{r},t)}{\partial t} \tag{19}$$

where $\hat{\boldsymbol{n}}$ is the outward normal to the surface $S'$.
Finally, the set of equations to be solved reads:

$$\boldsymbol{E}_0(\boldsymbol{r},t) = \frac{\boldsymbol{J}(\boldsymbol{r},t)}{\sigma} + \frac{\partial}{\partial t}\frac{\mu}{4\pi}\int_{V'}\frac{\boldsymbol{J}(\boldsymbol{r}',t')}{|\boldsymbol{r}-\boldsymbol{r}'|}dV' + \nabla\Phi(\boldsymbol{r},t) \tag{20a}$$

$$\Phi(\boldsymbol{r},t) = \frac{1}{4\pi\varepsilon}\int_{S'}\frac{\varrho(\boldsymbol{r}',t')}{|\boldsymbol{r}-\boldsymbol{r}'|}dS' \qquad \boldsymbol{r}\in S' \tag{20b}$$

$$\nabla\cdot\boldsymbol{J}(\boldsymbol{r},t) = 0 \qquad \boldsymbol{r}\in V' \tag{20c}$$

$$\hat{\boldsymbol{n}}\cdot\boldsymbol{J}(\boldsymbol{r},t) = \frac{\partial\varrho(\boldsymbol{r},t)}{\partial t} \qquad \boldsymbol{r}\in S' \tag{20d}$$

The unknowns of such a problem are represented by the current density $\boldsymbol{J}(\boldsymbol{r},t)$ in the interior of the conductors, the charge density $\varrho(\boldsymbol{r},t)$ on the surface of the conductors and the electric scalar potential distribution $\Phi(\boldsymbol{r},t)$ of conductors which can be directly expressed as a function of the charge density for $\boldsymbol{r} \in S'$.
Equations (20a)-(20d) can be rewritten in the Laplace domain as:

$$\boldsymbol{E}_0(\boldsymbol{r},s) = \frac{\boldsymbol{J}(\boldsymbol{r},s)}{\sigma} + \frac{s\mu}{4\pi}\int_{V'}\frac{\boldsymbol{J}(\boldsymbol{r}',s)\,e^{-s\tau}}{|\boldsymbol{r}-\boldsymbol{r}'|}dV' + \nabla\Phi(\boldsymbol{r},s) \tag{21a}$$

$$\Phi(\boldsymbol{r},s) = \frac{1}{4\pi\varepsilon}\int_{S'}\frac{\varrho(\boldsymbol{r}',s)\,e^{-s\tau}}{|\boldsymbol{r}-\boldsymbol{r}'|}dS' \qquad \boldsymbol{r}\in S' \tag{21b}$$

$$\nabla\cdot\boldsymbol{J}(\boldsymbol{r},s) = 0 \qquad \boldsymbol{r}\in V' \tag{21c}$$

$$\hat{\boldsymbol{n}}\cdot\boldsymbol{J}(\boldsymbol{r},s) = s\varrho(\boldsymbol{r},s) \qquad \boldsymbol{r}\in S' \tag{21d}$$

where $\tau = |\boldsymbol{r}-\boldsymbol{r}'|/c$ and $s$ is the Laplace variable.

The most popular method for the discretization of integral equations was called by Harrington the *method of moments* (MoM) [5] with different implementation [12]- [16]. Usually the solution is found in the frequency domain, assuming $s = j\omega$. As a first step the unknown quantities $\boldsymbol{J}(\boldsymbol{r},\omega)$ and $\varrho(\boldsymbol{r},\omega)$ are approximated by a weighted sum of finite set of basis functions $\boldsymbol{b}\in\mathcal{R}^3$ and $p\in\mathcal{R}$:

$$\boldsymbol{J}(\boldsymbol{r},\omega) \cong \sum_{n=1}^{N_v}\boldsymbol{b}_n(\boldsymbol{r})\,I_n(\omega) \tag{22a}$$

$$\varrho(\boldsymbol{r},\omega) \cong \sum_{m=1}^{N_s}p_m(\boldsymbol{r})\,Q_m(\omega) \tag{22b}$$

where $I_n(\omega)$ and $Q_m(\omega)$ are the basis function weights which must be determined at each angular frequency $\omega$, $N_v$ and $N_s$ represent the number of volume and surface basis functions and the corresponding elementary volume and surface sub-regions, respectively. Expansion (22a)-(22b) are substituted into (21a)-(21b), evaluated for $s = j\omega$, yielding:

$$\begin{aligned}\boldsymbol{E}_0(\boldsymbol{r},\omega) &= \sum_{n=1}^{N_v}\frac{\boldsymbol{b}_n(\boldsymbol{r})\,I_n(\omega)}{\sigma} + \frac{j\omega\mu}{4\pi}\sum_{n=1}^{N_v}\int_{V_n}\boldsymbol{b}_n(\boldsymbol{r}_n)\,I_n(\omega)\,\frac{e^{-j\omega\tau}}{|\boldsymbol{r}-\boldsymbol{r}_n|}dV_n + \\ &+ \nabla\Phi(\boldsymbol{r},\omega)\end{aligned} \tag{23a}$$

$$\Phi(\boldsymbol{r},\omega) = \frac{1}{4\pi\varepsilon}\sum_{m=1}^{N_s}\int_{S_m}p_m(\boldsymbol{r}_m)\,Q_m(\omega)\,\frac{e^{-j\omega\tau}}{|\boldsymbol{r}-\boldsymbol{r}_m|}dS_m \tag{23b}$$

Next, the so-called Galerkin's testing or weighting process ( [15]) is used to generate a system of equations for the unknowns weights $I_n(\omega), n = 1\cdots N_v$ and $Q_m(\omega), m = 1\cdots N_s$ by enforcing the residuals of equations (21a)-(21b) to be orthogonal to a set of weighting functions which are chosen to be coincident with the basis functions:

$$\begin{aligned}&\langle -\boldsymbol{E}_0(\boldsymbol{r},\omega) + \frac{\sum_{n=1}^{N_v}\boldsymbol{b}_n(\boldsymbol{r})\,I_n(\omega)}{\sigma} + \\ &\frac{j\omega\mu}{4\pi}\left(\sum_{n=1}^{N_v}\int_{V_n}\boldsymbol{b}_n(\boldsymbol{r}_n)\,I_n(\omega)\,\frac{e^{-j\omega\tau}}{|\boldsymbol{r}-\boldsymbol{r}_n|}\right)dV_n + \nabla\Phi(\boldsymbol{r},\omega), \boldsymbol{b}_i(\boldsymbol{r})\rangle = 0\end{aligned} \tag{24a}$$

$$\langle\Phi(\boldsymbol{r},\omega) - \frac{1}{4\pi\varepsilon}\sum_{m=1}^{N_s}\int_{S_m}p_m(\boldsymbol{r}_m)\,Q_m(\omega)\,\frac{e^{-j\omega\tau}}{|\boldsymbol{r}-\boldsymbol{r}_m|}dS_m, p_j(\boldsymbol{r})\rangle = 0 \tag{24b}$$

where the inner products are defined as:

$$\langle\boldsymbol{f}(\boldsymbol{r}),\boldsymbol{b}_i(\boldsymbol{r})\rangle = \int_{V_i}\boldsymbol{f}(\boldsymbol{r})\cdot\boldsymbol{b}_i(\boldsymbol{r})\,dV_i \qquad \text{for } i = 1\cdots N_v \tag{25a}$$

$$\langle g(\boldsymbol{r}),p_j(\boldsymbol{r})\rangle = \int_{S_j}g(\boldsymbol{r})\cdot p_j(\boldsymbol{r})\,dS_j \qquad \text{for } j = 1\cdots N_s \tag{25b}$$

*A. Choice of the basis and weighting functions for the conductor surfaces*

A number of different kind of basis and weighting functions can be chosen to set the equations (24a) and (24b). The most popular are the piecewise constant, piecewise linear, RWG [13] set of basis and/or weighting functions. In the following we will assume the piecewise constant set of functions which are more suited to model Manhattan type structures. Thus, we assume to deal with orthogonal conductors whose surface is discretized into $N_s$ elementary rectangular patches which are electrically small compared with the wavelength of the highest frequency of interest. More specifically, the unknown electrical current and charge densities are taken to have constant values over each cell in the discrete model.
Under this assumption the basis functions used to expand the charge density are chosen as:

$$p_m(\boldsymbol{r}) = \begin{cases} \frac{1}{S_m} & \text{if } \boldsymbol{r} \in S_m \\ 0 & \text{otherwise} \end{cases} \tag{26}$$

With such a choice of the basis function the corresponding weight $Q_m$ represents the charge on patch $m$. Finally, equation (23b) can be rewritten as

$$\Phi(\boldsymbol{r},\omega) = \sum_{m=1}^{N_s} \left[ \frac{1}{4\pi\varepsilon} \frac{1}{S_m} \int_{S_m} \frac{e^{-j\omega\tau}}{|\boldsymbol{r}-\boldsymbol{r}_m|} dS_m \right] Q_m(\omega) \tag{27}$$

which allows to evaluate the potential at point $\boldsymbol{r}$, at angular frequency $\omega$, due to the charge on the $N_s$ patches covering the conductors; in a sense such equation models the electric field coupling in the background medium with permittivity $\varepsilon$.

Applying the Galerkin scheme results in the evaluation of the average value of $\Phi(\boldsymbol{r},\omega)$ over the surface of each patch:

$$\begin{aligned} \Phi_l(\boldsymbol{r}_l,\omega) &= \frac{1}{S_l} \int_{S_l} \Phi(\boldsymbol{r}_l,\omega)\, dS_l = \\ &= \sum_{m=1}^{N_s} \left[ \frac{1}{4\pi\varepsilon} \frac{1}{S_l} \frac{1}{S_m} \int_{S_l} \int_{S_m} \frac{e^{-j\omega\tau}}{|\boldsymbol{r}_l-\boldsymbol{r}_m|} dS_m dS_l \right] Q_m(\omega) = \\ &= P_{lm}(\omega)\, Q_m(\omega) \qquad \text{for } l = 1 \cdots N_s \end{aligned} \tag{28}$$

where coefficient of potential $P_{lm}(\omega)$ is:

$$P_{lm}(\omega) = \frac{1}{4\pi\varepsilon} \frac{1}{S_l S_m} \int_{S_l} \int_{S_m} \frac{e^{-j\omega\tau}}{|\boldsymbol{r}_l-\boldsymbol{r}_m|} dS_m dS_l \tag{29}$$

Thus, the potential of the $N_s$ patches can be related to the charges located on the same patches, at the angular frequency $\omega$, by:

$$\boldsymbol{\Phi}(\omega) = \boldsymbol{P}(\omega)\, \boldsymbol{Q}(\omega) \tag{30}$$

where matrix $\boldsymbol{P}$ entries are known as coefficients of potential and are, in general frequency dependent due to the full wave type of analysis. The displacement currents in the background medium are obtained as:

$$\boldsymbol{I}_c(\omega) = j\omega \boldsymbol{Q}(\omega) = j\omega \boldsymbol{P}(\omega)^{-1} \boldsymbol{\Phi}(\omega) \tag{31}$$

*B. Choice of the basis and weighting functions for the conductor volumes*

Conductor volumes are discretized into $N_v$ elementary orthogonal hexahedra (parallelepiped) which are, as before, electrically small compared with the wavelength of the highest frequency of interest. Let $l_n$ and $a_n$ the length and the cross section of volume $V_n$, respectively.
The basis functions used to expand the current density are chosen as:

$$\boldsymbol{b}_n(\boldsymbol{r}) = \begin{cases} \frac{\hat{\boldsymbol{u}}_n}{a_n} & \text{if } \boldsymbol{r} \in V_n \\ \boldsymbol{0} & \text{otherwise} \end{cases} \tag{32}$$

where $\hat{\boldsymbol{u}}_n$ is the unit vector indicating the current orientation in volume $V_n$. With such a choice of the basis function the corresponding weight represents the current flowing in the volume $V_n$ with orientation $\hat{\boldsymbol{u}}_n$. Equation (23a), after the Galerkin scheme is applied, can be rewritten as:

$$\begin{aligned} E_0\left(\boldsymbol{r}_i,\omega\right) l_i &= \frac{l_i I_i\left(\omega\right)}{\sigma a_i} + \\ &+ \frac{j\omega\mu}{4\pi}\sum_{n=1}^{N_v}\frac{1}{a_i}\frac{1}{a_n}\int_{V_i}\int_{V_n}\hat{\boldsymbol{u}}_i\cdot\hat{\boldsymbol{u}}_n I_n\left(\omega\right)\frac{e^{-j\omega\tau}}{\left|\boldsymbol{r}_i-\boldsymbol{r}_n\right|}dV_n dV_i + \\ &+ \Phi_{2i}\left(\omega\right)-\Phi_{1i}\left(\omega\right) \qquad \text{for } i=1\cdots N_v \end{aligned} \tag{33}$$

In deriving the previous equation the external electric field $\boldsymbol{E}_0\left(\boldsymbol{r},\omega\right)$ has been assumed uniform in the volume $V_i$. Also, it has been considered that:

$$\begin{aligned} \frac{1}{a_i}\int_{V_i}\hat{\boldsymbol{u}}_i\cdot\nabla\Phi\left(\boldsymbol{r},\omega\right)dV_i &= \frac{1}{a_i}\int_{a_i}\left(\int_{l_i}\hat{\boldsymbol{u}}_i\cdot\nabla\Phi\left(\boldsymbol{r},\omega\right)dl_i\right)da_i = \\ &= \Phi_{2i}\left(\omega\right)-\Phi_{1i}\left(\omega\right) \end{aligned} \tag{34}$$

where $\Phi_{1i}\left(\omega\right)$ and $\Phi_{2i}\left(\omega\right)$ represent the potential at the extremes of the volume $V_i$ along the $\hat{\boldsymbol{u}}_i$ direction. Each term of equation (33) represents a voltage drop across volume $V_i$ along the $\hat{\boldsymbol{u}}_i$ direction and, thus, it can be rewritten as:

$$\Phi_{1i}\left(\omega\right)-\Phi_{2i}\left(\omega\right) = V_{0i}\left(\omega\right)+R_i I_i + j\omega\sum_{n=1}^{N_v}L_{p,in}I_n\left(\omega\right) \tag{35}$$

where

$$V_{0i}\left(\omega\right) = -E_0\left(\boldsymbol{r}_i,\omega\right)l_i \tag{36}$$

represents the voltage source due to external fields;

$$R_i = \frac{l_i}{\sigma a_i} \tag{37}$$

is the resistance of the cell $i$ where current flows along $l_i$;

$$L_{p,in}\left(\omega\right) = \frac{\mu}{4\pi}\frac{1}{a_i a_n}\int_{V_i}\int_{V_n}\hat{\boldsymbol{u}}_i\cdot\hat{\boldsymbol{u}}_n\frac{e^{-j\omega\tau}}{\left|\boldsymbol{r}_i-\boldsymbol{r}_n\right|}dV_n dV_i \tag{38}$$

is the so called partial inductance [17] between volume cells $i$ and $n$;

$$\Phi_{1i}\left(\omega\right)-\Phi_{2i}\left(\omega\right) \tag{39}$$

is the difference of potential between nodes at the extremes of volume $V_i$, along the $\hat{\boldsymbol{u}}_i$ direction.
In a more compact matrix form equation (35) can be written as:

$$-\boldsymbol{A}\boldsymbol{\Phi}\left(\omega\right)-\boldsymbol{R}\boldsymbol{I}_L\left(\omega\right)-j\omega\boldsymbol{L}_p\left(\omega\right)\boldsymbol{I}_L\left(\omega\right)-\boldsymbol{V}_0\left(\omega\right)=\boldsymbol{0} \tag{40}$$

where vectors $\boldsymbol{\Phi}$ and $\boldsymbol{I}_L$ collect the potentials to infinity and the currents flowing through the longitudinal branches, respectively and the matrix $A$ is the connectivity matrix whose entries are:

$$a_{nk} = \begin{cases} \text{+1 if current } I_{Ln} \text{ leaves node } k \\ \text{-1 if current } I_{Ln} \text{ enters node } k \\ \text{0 otherwise} \end{cases} \tag{41}$$

It is worth to notice that the discretization process described above has allowed to generate circuit topological elements such as branches, where currents $I_{Li}, i=1\cdots N_v$, flow and nodes, whose potential to infinity is $\Phi_l, l=1\cdots N$ where $N>N_s$ as, in the case of 3-D structures, nodes interior to the conductors may occur.

At this point the generation of equivalent circuits is straightforward, as described in the next Section.

## III. Development of Equivalent Circuit Models

The procedure outlined above has allowed to write equations (20a)-(20d) in such a way that circuit unknowns are used, namely currents $I_{Li}(\omega)$, $i = 1 \cdots N_v$, potentials $\Phi_l(\omega)$, $l = 1 \cdots N$ and charges $Q_m(\omega)$, $m = 1 \cdots N_s$. The synthesis of the equivalent circuit is best demonstrated through the application of the procedure to the very simple example of a zero thickness strip of conductor depicted in Fig. 1. The discretization process has been accomplished leading to three nodes, 1,2 and 3, and two branches, connecting them. The corresponding unknowns are the potential to infinity of the nodes, $\Phi_1$,$\Phi_2$ and $\Phi_3$, and the currents $I_{L1}$ and $I_{L2}$ flowing through the branches.

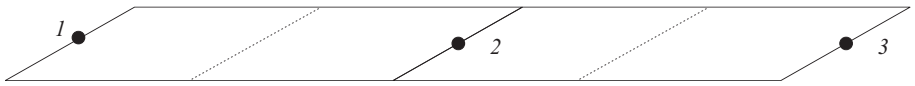


Fig. 1. Single zero thickness conductor with three nodes.

### A. Model for electric field coupling

A circuit model for the electric field coupling can be obtained stemming from equation (30) which, in the considered example, reads:

$$\Phi_1 = P_{11}Q_1 + P_{12}Q_2 + P_{13}Q_3 \tag{42a}$$
$$\Phi_2 = P_{21}Q_1 + P_{22}Q_2 + P_{23}Q_3 \tag{42b}$$
$$\Phi_3 = P_{31}Q_1 + P_{32}Q_2 + P_{33}Q_3 \tag{42c}$$

For implementation purposes in time domain it is useful to separate the self effect from the mutual effects. The displacement currents are obtained by taking the derivative of both the equations (42a)- (42c) yielding:

$$I_{c1} = j\omega Q_1 = j\omega\frac{1}{P_{11}}\Phi_1 - j\omega\frac{P_{12}}{P_{11}}Q_2 - j\omega\frac{P_{13}}{P_{11}}Q_3 \tag{43a}$$
$$I_{c2} = j\omega Q_2 = j\omega\frac{1}{P_{22}}\Phi_2 - j\omega\frac{P_{21}}{P_{22}}Q_1 - j\omega\frac{P_{23}}{P_{22}}Q_3 \tag{43b}$$
$$I_{c3} = j\omega Q_3 = j\omega\frac{1}{P_{33}}\Phi_3 - j\omega\frac{P_{31}}{P_{33}}Q_1 - j\omega\frac{P_{32}}{P_{33}}Q_2 \tag{43c}$$

which allows to identify the contribution of the self cell, which can be modelled as a capacitor, from the mutual coupling, which is modelled in terms of current controlled current sources (CCCSs) $I_1, I_2, I_3$ as:

$$I_1 = j\omega\frac{P_{12}}{P_{11}}Q_2 + j\omega\frac{P_{13}}{P_{11}}Q_3 \tag{44a}$$
$$I_2 = j\omega\frac{P_{21}}{P_{22}}Q_1 + j\omega\frac{P_{23}}{P_{22}}Q_3 \tag{44b}$$
$$I_3 = j\omega\frac{P_{31}}{P_{33}}Q_1 + j\omega\frac{P_{32}}{P_{33}}Q_2 \tag{44c}$$

In the most general case the $k-$th CCCS can be defined as:

$$I_k = \sum_{\substack{m=1 \\ m\neq k}}^{N_s}\frac{P_{km}}{P_{kk}}j\omega Q_m = \sum_{\substack{m=1 \\ m\neq k}}^{N_s}\frac{P_{km}}{P_{kk}}I_{c,m} \tag{45}$$

Thus, currents $\boldsymbol{I}$ are related to currents $\boldsymbol{I}_c$ by:

$$\boldsymbol{I} = \boldsymbol{T}\boldsymbol{I}_c \tag{46}$$

where

$$\boldsymbol{T} = \begin{bmatrix} 1 & \frac{p_{12}}{p_{11}} & \cdots & \frac{p_{1N_s}}{p_{11}} \\ \frac{p_{21}}{p_{22}} & 1 & \cdots & \frac{p_{2N_s}}{p_{22}} \\ \vdots & \vdots & \vdots & \vdots \\ \frac{p_{N_s1}}{p_{N_sN_s}} & \frac{p_{N_s2}}{p_{N_sN_s}} & \cdots & 1 \end{bmatrix} \tag{47}$$

Let's introduce a matrix $\boldsymbol{D}$ to describe the self induced effect as:

$$j\omega \boldsymbol{D}\boldsymbol{\Phi} \tag{48}$$

where

$$\boldsymbol{D} = \begin{bmatrix} \frac{1}{p_{11}} & 0 & \cdots & 0 \\ 0 & \frac{1}{p_{22}} & \cdots & 0 \\ \vdots & \vdots & \vdots & \vdots \\ 0 & 0 & \cdots & \frac{1}{p_{N_sN_s}} \end{bmatrix} \tag{49}$$

Equations (43a-43c) in a more compact form as:

$$\boldsymbol{I}_c = j\omega \boldsymbol{D}\boldsymbol{\Phi} - \boldsymbol{T}\boldsymbol{I}_c \tag{50}$$

Such equations are is well suited for a circuit interpretation, shown in Fig. 2.

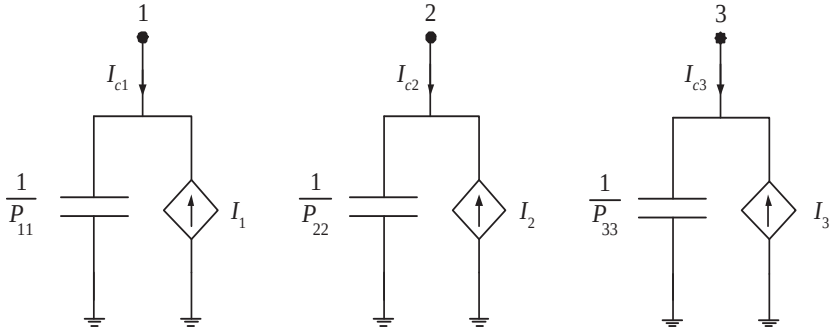


Fig. 2. Equivalent circuit model for electric field coupling.

Also, the following $\boldsymbol{P}$ matrix factorization can be established:

$$\boldsymbol{P}^{-1} = \boldsymbol{D}\boldsymbol{S}^{-1} \tag{51}$$

where matrix $\boldsymbol{S}$ is defined as:

$$\boldsymbol{S} = \begin{bmatrix} 1 & \frac{p_{12}}{p_{22}} & \cdots & \frac{p_{1N_s}}{p_{N_sN_s}} \\ \frac{p_{21}}{p_{11}} & 1 & \cdots & \frac{p_{2N_s}}{p_{N_sN_s}} \\ \vdots & \vdots & \vdots & \vdots \\ \frac{p_{N_s1}}{p_{11}} & \frac{p_{N_s2}}{p_{22}} & \cdots & 1 \end{bmatrix} \tag{52}$$

It is easy to verify that the following identity holds:

$$\boldsymbol{S} = \boldsymbol{T}^t \tag{53}$$

It has to be pointed out that equations (42a)- (42b) allow to model the electric field coupling in the background medium.

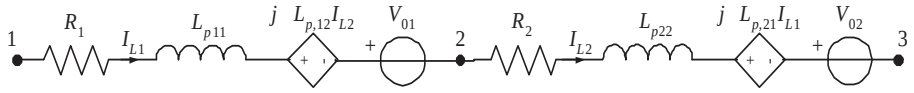


Fig. 3. Equivalent circuit model for magnetic field coupling.

### *B. Model for magnetic field coupling*

A circuit model for the magnetic field coupling can be obtained stemming from equation (33) which, enforcing the electric field equation (5) in a discrete form, in the considered example reads:

$$\Phi_1 - \Phi_2 = (R_1 + j\omega L_{p11} I_{L1} + j\omega L_{p12} I_2 + V_{01}) \tag{54a}$$

$$\Phi_2 - \Phi_3 = (R_2 + j\omega L_{p22} I_{L2} + j\omega L_{p21} I_1 + V_{02}) \tag{54b}$$

It is suited for the circuit synthesis shown in Fig. 3
In the considered example no interior node occurs, thus $N_s = N = 3$.

### *C. PEEC equivalent circuit*

Once the equivalent circuits for the electric and magnetic field coupling have been generated, the next task is to connect equivalent circuits shown in Figs. 2 and 3. This can be accomplished just by connecting nodes 1,2 and 3 in Figs. 2 and 3, thus leading to the equivalent circuit sketched in Fig. 4.

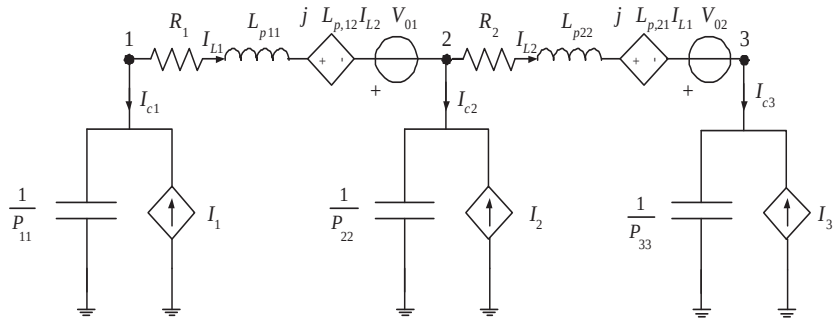


Fig. 4. Equivalent circuit model for the simple example in Fig. 1.

### *D. Enforcement of Kirchhoff's current and voltage laws*

Once the equivalent circuit is generated, Kirchhoff's current and voltage laws can be enforced. The first set of equation can be obtained by enforcing Kirchhoff's voltage law (KVL) applied to a mesh constituted by the resistive-inductive branch connecting each couple of nodes and the capacitive branch connecting each node to infinity. It yields the set of equations (40), here repeated for the sake of clarity,

$$-\boldsymbol{A}\boldsymbol{\Phi}(\omega) - \boldsymbol{R}\boldsymbol{I}(\omega) - j\omega\boldsymbol{L}_p(\omega)\boldsymbol{I}(\omega) - \boldsymbol{V}_0(\omega) = \boldsymbol{0} \tag{55}$$

The PEEC method enforces the continuity equation in the form of Kirchhoff's current law (KCL); taking into account that both $\boldsymbol{I}_L$ and $\boldsymbol{I}_c$ and that external current sources $\boldsymbol{I}_s$ can be connected to each node, KCL can be written as:

$$\boldsymbol{I}_c(\omega) - \boldsymbol{A}^t\boldsymbol{I}_L(\omega) = \boldsymbol{I}_s(\omega) \tag{56}$$

where $t$ denotes transpose. Considering that the displacement currents $\boldsymbol{I}_c$ can be expressed as a function of the potentials $\boldsymbol{\Phi}$ (31), it is possible to write:

$$j\omega\boldsymbol{P}(\omega)^{-1}\boldsymbol{\Phi}(\omega) - \boldsymbol{A}^t\boldsymbol{I}_L(\omega) = \boldsymbol{I}_s(\omega) \tag{57}$$

From the implementation point of view it may be desirable to avoid the matrix inversion $\boldsymbol{P}(\omega)^{-1}$ because of its complexity ($O(n^3)$). Matrix $\boldsymbol{P}(\omega)$ can be used as preconditioner, allowing to re-write the previous equation as:

$$j\omega\boldsymbol{\Phi}(\omega) - \boldsymbol{P}(\omega)\boldsymbol{A}^t\boldsymbol{I}_L(\omega) = \boldsymbol{P}(\omega)\boldsymbol{I}_s(\omega) \tag{58}$$

## IV. Computation of partial elements

As seen in the previous Section, building a PEEC model requires computing partial elements, namely partial inductances, coefficients of potential, describing the magnetic and electric couplings respectively and resistances which account for power dissipation in conductive materials. The present Section focuses on the computation of partial elements and existing closed formulas which allow fast and accurate partial elements computation.

### *A. Computation of partial inductances*

The evaluation of partial inductances requires the computation of double folded volume integrals as (38):

$$L_{p,in}(\omega) = \frac{\mu}{4\pi}\frac{1}{a_i a_n}\int_{V_i}\int_{V_n} \hat{\boldsymbol{u}}_i \cdot \hat{\boldsymbol{u}}_n \frac{e^{-j\omega\tau}}{|\boldsymbol{r}_i - \boldsymbol{r}_n|} dV_n dV_i \tag{59}$$

If the discretization matches the $\lambda_{min}/20$ rule (max(dim)$<$ $\lambda_{min}/20$), being max(dim) the maximum dimension of cells and $lambda_{min}$ the minimum wavelength of interest, a center to center approximation can be assumed and the partial inductance can be computed as

$$L_{p,in}(\omega) = \frac{\mu}{4\pi}\frac{e^{-j\omega\tau_{in}^{cc}}}{a_i a_n}\int_{V_i}\int_{V_n} \hat{\boldsymbol{u}}_i \cdot \hat{\boldsymbol{u}}_n \frac{1}{|\boldsymbol{r}_i - \boldsymbol{r}_n|} dV_n dV_i = L_{p,in}^{st} e^{-j\omega\tau_{in}^{cc}} \tag{60}$$

where $\tau_{in}^{cc}$ is the center to center distance between volume cells $i$ and $n$.

For general geometries and not negligible delays numerical integration techniques must used. In the quasi-static case and orthogonal geometry analytical formulas are available. In the following a review of partial inductances computation techniques is presented. A more detailed description of closed formula for partial inductances evaluation for standard configurations can be found in [17]- [19].

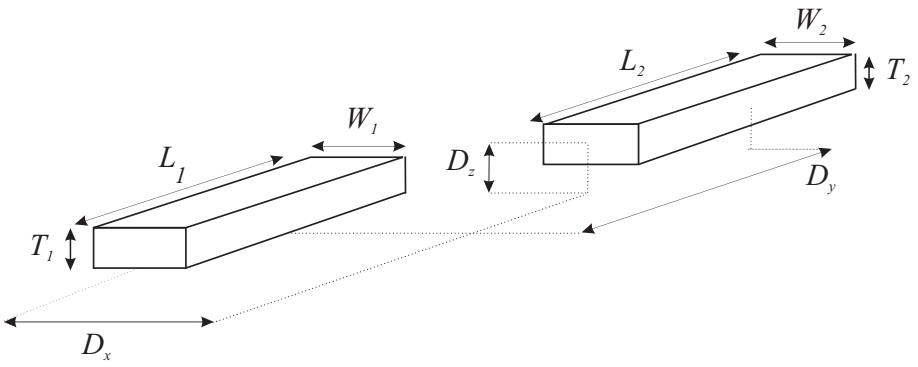


Fig. 5. Geometry and notation for the computation of self and mutual partial inductances.

*a) Self Partial Inductance of a 3D rectangular cell:*

$$\begin{aligned}
\frac{Lp_{ii}}{L} &= \frac{2\mu}{\pi}\{\frac{\omega^2}{24u}\left[\ln(\frac{1+A_2}{\omega}) - A_5\right] + \frac{1}{24u\omega}\left[\ln(\omega + A_2) - A_6\right] \\
&+\frac{\omega^2}{60u}(A_4 - A_3) + \frac{\omega^2}{24}[\ln(\frac{u+A_3}{\omega}) - A_7] + \frac{\omega^2}{60u}(\omega - A_2) + \frac{1}{20u}(A_2 - A_4) \\
&+\frac{u}{4}A_5 - \frac{u^2}{6\omega}\tan^{-1}(\frac{\omega}{uA_4}) + \frac{u}{4\omega}A_6 - \frac{\omega}{6}\tan^{-1}(\frac{u}{\omega A_4}) + \frac{A_7}{4} \\
&-\frac{1}{6\omega}\tan^{-1}(\frac{u\omega}{A_4}) + \frac{1}{24\omega^2}\left[\ln(u + A_1) - A_7\right] + \frac{u}{20\omega^2}(A_1 - A_4) \\
&+\frac{1}{60\omega^2 u}(1 - A_2) + \frac{1}{60u\omega^2}(A_4 - A_1) + \frac{u}{20}(A_3 - A_4) \\
&+\frac{u^3}{24\omega^2}\left[\ln(\frac{1+A_1}{u}) - A_5\right] + \frac{u^3}{24\omega}\left[\ln(\frac{\omega + A_3}{u}) - A_6\right] \\
&+\frac{u^3}{60\omega^2}\left[(A_4 - A_1) + (u - A_3)\right]\}
\end{aligned} \tag{61}$$

where $u = L/W$, $\omega = T/W$ and the following notation is adopted:

$$\begin{aligned} A_1 &= \sqrt{1+u^2} \quad A_2 = \sqrt{1+\omega^2} \\ A_3 &= \sqrt{\omega^2+u^2} \quad A_4 = \sqrt{1+\omega^2+u^2} \\ A_5 &= \ln\left(\frac{1+A_4}{A_3}\right) \quad A_6 = \ln\left(\frac{\omega+A_4}{A_1}\right) \end{aligned} \tag{62}$$

$$A_7 = \ln\left(\frac{u+A_4}{A_2}\right) \tag{63}$$

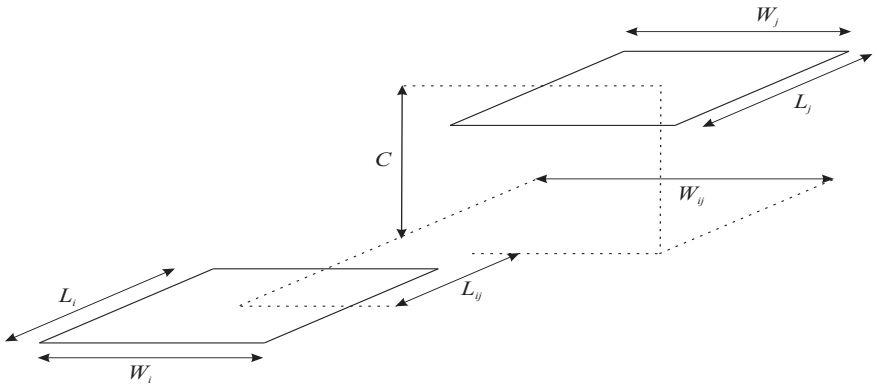


Fig. 6. Co-planar zero-thickness conductor geometry for the evaluation of the mutual partial inductance and coefficient of potential.

*b) Mutual partial inductance of 2D rectangular cells:*

$$\begin{aligned} L_{p,ij} &= \frac{\mu}{4\pi}\frac{1}{W_i W_j}\sum_{k=1}^{4}\sum_{m=1}^{4}(-1)^{m+k}\left[\frac{b_m^2-C^2}{2}a_k\,\ln(a_k+\rho)\right. \\ &\quad \left. + \frac{a_k^2-C^2}{2}b_m\,\ln(b_m+\rho) - \frac{1}{6}(b_m^2-2C^2+a_k^2)\rho - b_m\,C\,a_k\tan^{-1}\frac{a_k\,b_m}{\rho\,C}\right] \end{aligned} \tag{64}$$

where

$$\rho = (a_k^2+b_m^2+C^2)^{\frac{1}{2}}$$

$$\begin{aligned} a_1 &= W_{ij} - \frac{W_i}{2} - \frac{W_j}{2}, \qquad a_2 = W_{ij} + \frac{W_i}{2} - \frac{W_j}{2} \\ a_3 &= W_{ij} + \frac{W_i}{2} + \frac{W_j}{2}, \qquad a_4 = W_{ij} - \frac{W_i}{2} + \frac{W_j}{2} \\ b_1 &= L_{ij} - \frac{L_i}{2} - \frac{L_j}{2}, \qquad b_2 = L_{ij} + \frac{L_i}{2} - \frac{L_j}{2} \\ b_3 &= L_{ij} + \frac{L_i}{2} + \frac{L_j}{2}, \qquad b_4 = L_{ij} - \frac{L_i}{2} + \frac{L_j}{2} \end{aligned}$$

and $C$ is the distance between the two planes containing surface cell $i$ and $j$.

*c) Mutual and self partial inductance of 1D rectangular cells:* In the case of structures where two dimensions are much smaller than the third, volumetric cells can be approximated as filaments. In such hypothesis a closed formula for mutual partial inductance between parallel filaments with equal length.

$$L_{pij} = \frac{\mu}{2\pi}L\left[\ln\left(\frac{L}{D}+\sqrt{\left(\frac{L}{D}\right)^2+1}\right) + \frac{D}{L} - \sqrt{\left(\frac{D}{L}\right)^2+1}\right] \tag{65}$$

A good approximation of the self partial inductance can be obtained by substituting $d$ with the radius $r$ of conductors:

$$L_{pii} = \frac{\mu}{2\pi}L\left[\ln\left(\frac{L}{r}+\sqrt{\left(\frac{L}{r}\right)^2+1}\right) + \frac{r}{L} - \sqrt{\left(\frac{r}{L}\right)^2+1}\right] \tag{66}$$

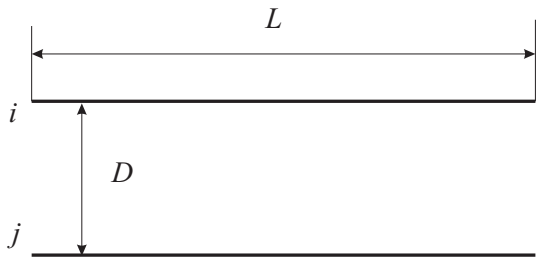


Fig. 7. Two parallel filaments.

### *B. Computation of coefficients of potential*

The evaluation of coefficients of potential requires the computation of double folded surface integrals as (29):

$$P_{lm}(\omega) = \frac{1}{4\pi\varepsilon}\frac{1}{S_l S_m}\int_{S_l}\int_{S_m}\frac{e^{-j\omega\tau}}{|\boldsymbol{r}_l - \boldsymbol{r}_m|}dS_m dS_l \tag{67}$$

As before, if the discretization matches the $\lambda_{min}/20$ rule, a center to center approximation can be assumed and the coefficient of potential can be computed as

$$P_{lm}(\omega) = \frac{1}{4\pi\varepsilon}\frac{e^{-j\omega\tau_{lm}^{cc}}}{S_l S_m}\int_{S_l}\int_{S_m}\frac{1}{|\boldsymbol{r}_l - \boldsymbol{r}_m|}dS_m dS_l = P_{lm}^{st}e^{-j\omega\tau_{lm}^{cc}} \tag{68}$$

where $\tau_{lm}^{cc}$ is the center to center distance between surface cells $l$ and $m$.

Obviously, for general geometries no closed-formula exists for such integrals and numerical integration is needed. In the quasi-static case and for selected geometry closed-formula can be adopted. To obtain good accuracy and fast evaluation of the partial coefficients of potential basic geometries, building blocks, have been defined. For each basic geometry a formulation for the evaluation of the partial coefficient of potential is given. The most important basic geometry is the *rectangular surface cell* depicted in Fig. 8. The interested reader may refer to [20], [21] for a complete overview of coefficients of potential computation.

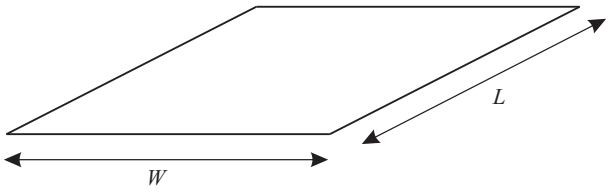


Fig. 8. Rectangular conductor geometry for the evaluation of the self coefficient of potential.

*d) Partial Self Coefficient of Potential:* The formula for the evaluation of the partial self coefficient of potential for the general rectangular conductor, equation (69), is given by a modified version of (16) in [17] which is used for the evaluation of the partial self inductance for thin conductors:

$$\begin{aligned} p_{ii} &= \frac{L}{4\pi\varepsilon}\frac{2}{3}\left\{ 3\,ln[u + (u^2+1)^{\frac{1}{2}}] + u^2 + \frac{1}{u}\right. \\ &+ \left. 3\,u\,ln\left[\frac{1}{u} + (\frac{1}{u^2}+1)^{\frac{1}{2}}\right] - \left[u^{\frac{4}{3}} + (\frac{1}{u})^{\frac{2}{3}}\right]^{\frac{3}{2}}\right\} \end{aligned} \tag{69}$$

where $u = L/W$ using the definitions from Fig. 8.

*e) Partial Mutual Coefficients of Potential:* Effective calculation routines for partial mutual coefficients of potential are, as for the partial inductances, more important than for partial self coefficients of potential due to the mutual capacitive/electric field coupling of all surface cells in the discretization. For the partial mutual coefficients of potential calculations two basic geometries has been defined to speed up and retain

good accuracy in the partial element calculations. The most important basic geometry is the mutual coupling between two rectangular surface cells, Fig. 6. The formula for the evaluation of the partial mutual coefficient of potential for the general conductor configuration in Fig. 6 is given by a modified version of the (64) used for partial mutual inductances for zero-thickness conductors. The equation uses the notations in Fig. 6 and is given by

$$\begin{aligned} p_{ij} &= \frac{1}{4\pi\varepsilon}\frac{1}{W_i L_i W_j L_j}\sum_{k=1}^{4}\sum_{m=1}^{4}(-1)^{m+k}\left[\frac{b_m^2-C^2}{2}a_k\,\ln(a_k+\rho)\right. \\ &\left. + \frac{a_k^2-C^2}{2}b_m\,\ln(b_m+\rho) - \frac{1}{6}(b_m^2-2C^2+a_k^2)\rho - b_m\,C\,a_k\tan^{-1}\frac{a_k\,b_m}{\rho\,C}\right] \end{aligned} \tag{70}$$

where

$$\rho = (a_k^2+b_m^2+C^2)^{\frac{1}{2}}$$

$$\begin{aligned} a_1 &= W_{ij}-\frac{W_i}{2}-\frac{W_j}{2}, & a_2 &= W_{ij}+\frac{W_i}{2}-\frac{W_j}{2} \\ a_3 &= W_{ij}+\frac{W_i}{2}+\frac{W_j}{2}, & a_4 &= W_{ij}-\frac{W_i}{2}+\frac{W_j}{2} \\ b_1 &= L_{ij}-\frac{L_i}{2}-\frac{L_j}{2}, & b_2 &= L_{ij}+\frac{L_i}{2}-\frac{L_j}{2} \\ b_3 &= L_{ij}+\frac{L_i}{2}+\frac{L_j}{2}, & b_4 &= L_{ij}-\frac{L_i}{2}+\frac{L_j}{2} \end{aligned}$$

and $C$ is the distance between the two planes containing surface cell $i$ and $j$.
The second basic geometry considered is that of two cells oriented perpendicular to each other as seen in Fig. 9.

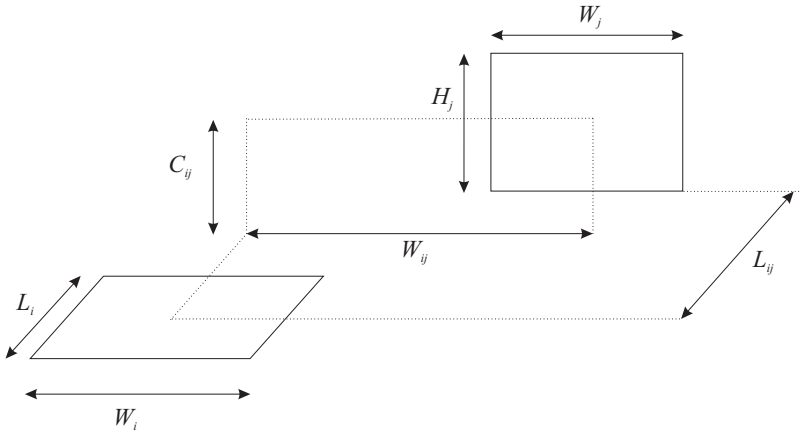


Fig. 9. Orthogonal Rectangular surface conductor geometry for the evaluation of the partial mutual coefficient of potential.

The evaluation of the perpendicular surface cell partial mutual coefficient of potential is given by equation (16) in [20].

$$\begin{aligned} p_{ij} &= \frac{1}{4\pi\varepsilon}\frac{1}{W_i L_i W_j H_j}\sum_{k=1}^{4}\sum_{m=1}^{2}\sum_{l=1}^{2}(-1)^{l+m+k+1}\,. \\ &\cdot \left[\left(\frac{a_k^2}{2}-\frac{c_l^2}{6}\right)c_l\ln(b_m+\rho)+\ldots\left(\frac{a_k^2}{2}-\frac{b_m^2}{6}\right)b_m\ln(c_l+\rho)+a_k b_m c_l\ln(a_k+\rho)\right. \\ &- \left.\frac{b_m c_l}{3}\rho-\frac{a_k^3}{6}\arctan\left(\frac{b_m c_l}{a_k\rho}\right)-\frac{b_m^2 a_k}{6}\arctan\left(\frac{a_k c_l}{b_m\rho}\right)-\frac{a_k c_l^2}{2}\arctan\left(\frac{a_k b_m}{c_l\rho}\right)\right] \end{aligned}$$

where

$$\rho = (a_k^2+b_m^2+C_{ij}^2)^{\frac{1}{2}}$$

$$
\begin{aligned}
a_1 &= W_{ij} - \frac{W_i}{2} - \frac{W_j}{2}, \quad a_2 = W_{ij} + \frac{W_i}{2} - \frac{W_j}{2} \\
a_3 &= W_{ij} + \frac{W_i}{2} + \frac{W_j}{2}, \quad a_4 = W_{ij} - \frac{W_i}{2} + \frac{W_j}{2} \\
b_1 &= L_{ij} + \frac{L_i}{2}, \qquad\qquad b_2 = L_{ij} - \frac{L_i}{2} \\
c_1 &= C_{ij} + \frac{H_j}{2}, \qquad\qquad c_1 = C_{ij} - \frac{H_j}{2}
\end{aligned}
$$

*Resistances*

The partial resistances in a PEEC model is calculated using the volume cell discretization and the resistance formula from (37) as:

$$R_\gamma = \frac{l_\gamma}{a_\gamma \sigma_\gamma} \tag{71}$$

where $l_\gamma$ is the length of the volume cell in the current direction, $a_\gamma$ is the cross section normal to the current direction, and $\sigma_\gamma$ is the conductivity of the volume cell material.

The resistance in the PEEC models accounts for the losses in the conductors. A more general approach to the computation of partial elements for non-orthogonal geometries can be found in [22], [23].

## V. Dielectrics Modeling

The key idea for modeling dielectrics is to represent the displacement current due to the bound charges for dielectrics with $\varepsilon_r > 1$ separately from the conducting currents due to the free charges. Maxwell's equation for the displacement current is written as:

$$\nabla \cdot \boldsymbol{E} = \frac{\varrho^F + \varrho^B}{\varepsilon_0} \tag{72}$$

where $\varrho^F$ is the free charge and $\varrho^B$ is the bound charge due to the dielectric regions. Thus, the global charge is: $\varrho^T = \varrho^F + \varrho^B$.

The dielectric volumes can be taken into account in terms of the polarization current density associated with their presence. This can be accomplished by adding and subtracting the displacement current in the background medium $\varepsilon_0 \varepsilon_r \frac{\partial \boldsymbol{E}(\boldsymbol{r},t)}{\partial t}$ in the Maxwell equation for $\boldsymbol{H}$ [24]:

$$
\begin{aligned}
\nabla \times \boldsymbol{H}(\boldsymbol{r},t) &= \boldsymbol{J}^C(\boldsymbol{r},t) + \varepsilon_0 \varepsilon_r \frac{\partial \boldsymbol{E}(\boldsymbol{r},t)}{\partial t} \\
&= \boldsymbol{J}^C(\boldsymbol{r},t) + \varepsilon_0(\varepsilon_r - 1)\frac{\partial \boldsymbol{E}(\boldsymbol{r},t)}{\partial t} + \varepsilon_0 \frac{\partial \boldsymbol{E}(\boldsymbol{r},t)}{\partial t}
\end{aligned} \tag{73}
$$

Thus, the total current in the equation (73) takes into account both the electric current related to the conductivity of the medium as well as the polarization current due to the dielectrics:

$$\boldsymbol{J}^T(\boldsymbol{r},t) = \boldsymbol{J}^C(\boldsymbol{r},t) + \varepsilon_0(\varepsilon_r - 1)\frac{\partial \boldsymbol{E}(\boldsymbol{r},t)}{\partial t} = \boldsymbol{J}^C(\boldsymbol{r},t) + \boldsymbol{J}^D(\boldsymbol{r},t) \tag{74}$$

Thus, the magnetic vector potential at point $\boldsymbol{r}$, given in (11) becomes:

$$\boldsymbol{A}(\boldsymbol{r},t) = \frac{\mu}{4\pi}\int_{V'} \frac{\boldsymbol{J}^T(\boldsymbol{r}',t')}{|\boldsymbol{r}-\boldsymbol{r}'|} dV' \tag{75}$$

For a point located in a conductor (20a) reads:

$$
\begin{aligned}
\boldsymbol{E}_0(\boldsymbol{r},t) &= \frac{\boldsymbol{J}^C(\boldsymbol{r},t)}{\sigma} + \frac{\partial}{\partial t}\frac{\mu}{4\pi}\int_{V'} \frac{\boldsymbol{J}^C(\boldsymbol{r}',t')}{|\boldsymbol{r}-\boldsymbol{r}'|} dV' \\
&+ \varepsilon_0(\varepsilon_r - 1)\frac{\mu}{4\pi}\int_{V'} \frac{1}{|\boldsymbol{r}-\boldsymbol{r}'|}\frac{\partial^2 \boldsymbol{E}(\boldsymbol{r}',t')}{\partial t^2} dV' \\
&+ \nabla\Phi(\boldsymbol{r},t)
\end{aligned} \tag{76}
$$

At a point $\boldsymbol{r}$ inside a dielectric region with relative permittivity $\varepsilon_r$ (20a) becomes:

$$\begin{aligned}\boldsymbol{E}_0(\boldsymbol{r},t) &= \boldsymbol{E}(\boldsymbol{r},t)+\frac{\partial}{\partial t}\frac{\mu}{4\pi}\int_{V'}\frac{\boldsymbol{J}^T(\boldsymbol{r}',t')}{|\boldsymbol{r}-\boldsymbol{r}'|}dV' \\ &+ \varepsilon_0(\varepsilon_r-1)\frac{\mu}{4\pi}\int_{V'}\frac{1}{|\boldsymbol{r}-\boldsymbol{r}'|}\frac{\partial^2\boldsymbol{E}(\boldsymbol{r}',t')}{\partial t^2}dV' \\ &+ \nabla\Phi(\boldsymbol{r},t)\end{aligned} \tag{77}$$

where $\Phi(\boldsymbol{r},t)$ is:

$$\Phi(\boldsymbol{r},t) = \frac{1}{4\pi\varepsilon}\int_{S'}\frac{\varrho^T(\boldsymbol{r}',t')}{|\boldsymbol{r}-\boldsymbol{r}'|}dS' \qquad \boldsymbol{r}\in S' \tag{78}$$

Thus, it can be observed that the electric field at a point $\boldsymbol{r}$, $\boldsymbol{E}(\boldsymbol{r})$, is determined by the first time derivative of the current density distribution $\boldsymbol{J}^T(\boldsymbol{r},t)$, the gradient of the electric scalar potential $\nabla\Phi(\boldsymbol{r},t)$ but also by the second derivative of the electric field itself $\partial^2\boldsymbol{E}(\boldsymbol{r}',t')/\partial t^2$.

As stated before the charges, $\varrho^F$, $\varrho^B$ and $\varrho^T$ are on the surface of the conductors and dielectrics while the currents flow through volumes. The continuity equation cannot be enforced as in the conventional moment type solutions [5]

$$\nabla\cdot\boldsymbol{J}^T+\frac{\partial\varrho^T}{\partial t}=0 \tag{79}$$

but it will implemented in the form of Kirchhoff's current law enforced to each node. Thus, within each conductor and each homogeneous block of dielectric we have:

$$\nabla\cdot\boldsymbol{J}^C(\boldsymbol{r}) = 0 \tag{80}$$

$$\nabla\cdot\boldsymbol{J}^D(\boldsymbol{r}) = 0 \tag{81}$$

Furthermore, on each conductor and dielectric the current normal to the surface causes accumulation of surface charge:

$$\hat{\boldsymbol{n}}\cdot\boldsymbol{J}^C(\boldsymbol{r}) = j\omega\varrho^F(\boldsymbol{r}) \tag{82}$$

$$\hat{\boldsymbol{n}}\cdot\boldsymbol{J}^D(\boldsymbol{r}) = j\omega\varrho^B(\boldsymbol{r}) \tag{83}$$

On the surface between touching conductor and dielectric blocks, equation (82) becomes:

$$\hat{\boldsymbol{n}}\cdot\boldsymbol{J}^T(\boldsymbol{r}) = j\omega\varrho^T(\boldsymbol{r}) \tag{84}$$

Let's refer to Fig. 10. We divide the conductors and dielectrics into blocks for which the conduction or displacement currents are assumed to be uniform. Further, the surfaces of conductors and dielectrics are completely laid out with panels to represent free and bound charges, respectively.

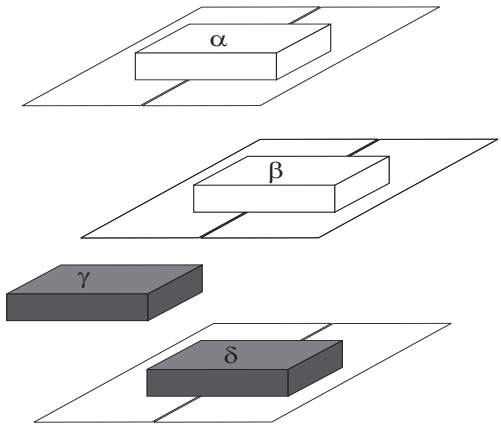


Fig. 10. Cell structure for finite conductors and dielectrics.

Cells $\alpha$ e $\beta$ represent conductors and free charge $\varrho^F$ is located on their surfaces. Dielectric cell $\gamma$ is an internal cell and has no outside surface; there is no charge on its surface; finally, dielectric cell $\delta$ is on the surface of the dielectric body and presents bound charge $\varrho^B$ on its surface. In the following we will refer to the total charge $\varrho^T$ to be general.

We can represent the vector quantities in terms of the Cartesian coordinates. For this case the vector quantities are $\boldsymbol{J} = J_x\hat{\boldsymbol{x}} + J_y\hat{\boldsymbol{y}} + J_z\hat{\boldsymbol{z}}$ and $\boldsymbol{E} = E_x\hat{\boldsymbol{x}} + E_y\hat{\boldsymbol{y}} + E_z\hat{\boldsymbol{z}}$. The three integral equations are identical in form with the exception of the space directions $x, y$ and $z$. We will consider cells in the $y$-direction only, without loss of generality Equations (76), (77) become three coupled integral equations. Vectors $\boldsymbol{r}$ e $\boldsymbol{r}'$ indicate the point where the electric field is evaluated and where the source, current or charge, is located, respectively. Two different cases must be considered depending on the location of the field point $\boldsymbol{r}$. In the first case the field point $\boldsymbol{r}$ is located in a conductor, in the second one it is in a dielectric block.

Let's assume first that $\boldsymbol{r}$ is located in a conductor cell and no external field $\boldsymbol{E}_0$ exists: equation (76) applied to the conductor cell $\alpha$ is:

$$\begin{aligned}
\frac{J_y^C(\boldsymbol{r},t)}{\sigma_\alpha} &+ \frac{\partial}{\partial t}\frac{\mu}{4\pi}\int_{V_{\alpha'}}\frac{J^C(\boldsymbol{r}',t')}{|\boldsymbol{r}-\boldsymbol{r}'|}dV'_\alpha \\
&+ \frac{\partial}{\partial t}\frac{\mu}{4\pi}\int_{V'_\beta}\frac{J^C(\boldsymbol{r}',t')}{|\boldsymbol{r}-\boldsymbol{r}'|}dV'_\beta \\
&+ \varepsilon_0(\varepsilon_\gamma-1)\frac{\mu}{4\pi}\int_{V'_\gamma}\frac{1}{|\boldsymbol{r}-\boldsymbol{r}'|}\frac{\partial^2 E_y(\boldsymbol{r}',t')}{\partial t^2}dV'_\gamma \\
&+ \varepsilon_0(\varepsilon_\delta-1)\frac{\mu}{4\pi}\int_{V'_\delta}\frac{1}{|\boldsymbol{r}-\boldsymbol{r}'|}\frac{\partial^2 E_y(\boldsymbol{r}',t')}{\partial t^2}dV'_\delta \\
&+ \frac{1}{4\pi\epsilon_0}\int_{S'_\alpha}\frac{\partial}{\partial y}\frac{1}{|\boldsymbol{r}-\boldsymbol{r}'|}\varrho^T(\boldsymbol{r}',t')dS'_\alpha \\
&+ \frac{1}{4\pi\epsilon_0}\int_{S'_\beta}\frac{\partial}{\partial y}\frac{1}{|\boldsymbol{r}-\boldsymbol{r}'|}\varrho^T(\boldsymbol{r}',t')dS'_\beta \\
&+ \frac{1}{4\pi\epsilon_0}\int_{S'_\delta}\frac{\partial}{\partial y}\frac{1}{|\boldsymbol{r}-\boldsymbol{r}'|}\varrho^T(\boldsymbol{r}',t')dS'_\delta = 0
\end{aligned} \tag{85}$$

where $\sigma_\alpha$ represents the electrical conductivity of cell $\alpha$.

Applying the Galerkin solution each single term of (85) has a circuit interpretation. In the following we assume that density current $J_y^C$ is uniform across the cross section of cell $\alpha$. Further, for the sake of clarity, we assume the quasi-static assumption, e.g. $t = t'$, thus neglecting the delay due to the speed of light in the background medium. The first term of (85) represents the voltage drop across the resistance of the cell $\alpha$:

$$\frac{1}{a_\alpha}\int_{V_\alpha}\frac{J_y^C(\boldsymbol{r}_\alpha,t)}{\sigma_\alpha}dV_\alpha = \frac{1}{a_\alpha}\int_{a_\alpha}\int_{l_\alpha}\frac{J_y^C(\boldsymbol{r}_\alpha,t)}{\sigma_\alpha}da_\alpha dl_\alpha = \rho_\alpha\frac{l_\alpha}{a_\alpha}(a_\alpha J_y^C) = R_\alpha I_y^C \tag{86}$$

The second term is the voltage drop across the self inductance of the cell $\alpha$:

$$\left(\frac{\mu}{4\pi a_\alpha a_\alpha}\int_{V'_\alpha}\int_{V_\alpha}\frac{1}{|\boldsymbol{r}_\alpha-\boldsymbol{r}'_\alpha|}dV'_\alpha dV_\alpha\right)\frac{d}{dt}(a_\alpha J_y^C) = L_{p\alpha\alpha}\frac{dI_y^C}{dt} \tag{87}$$

This allows to identify the self partial inductance of cell $\alpha$ as:

$$L_{p\alpha\alpha} = \frac{\mu}{4\pi a_\alpha a_\alpha}\int_{V'_\alpha}\int_{V_\alpha}\frac{1}{|\boldsymbol{r}_\alpha-\boldsymbol{r}'_\alpha|}dV'_\alpha dV_\alpha \tag{88}$$

Following the same procedure it is possible to recognize in the third term of (85) the mutual partial inductance between the conductor cells $\alpha$ e $\beta$:

$$L_{p\alpha\beta} = \frac{\mu}{4\pi a_\alpha a_\beta}\int_{V_\alpha}\int_{V_\beta}\frac{1}{|\boldsymbol{r}_\alpha-\boldsymbol{r}_\beta|}dV_\alpha dV_\beta \tag{89}$$

The fourth and fifth terms model the coupling among the conductor cell $\alpha$ and dielectric cells $\gamma$ e $\delta$: as clearly seen, although the different nature of materials, such term still represents an inductive coupling:

$$\begin{aligned}
&\varepsilon_0(\varepsilon_\gamma - 1)\frac{\mu}{4\pi a_\alpha}\int_{V_\alpha}\int_{V'_\gamma}\frac{1}{|\boldsymbol{r}_\alpha - \boldsymbol{r}'_\gamma|}\frac{\partial^2 E_y(\boldsymbol{r}'_\gamma, t_d)}{\partial t^2}dV'_\gamma dV_\alpha = \\
&= \left(\frac{\mu}{4\pi a_\alpha}\int_{V_\alpha}\int_{V_\gamma}\frac{1}{|\boldsymbol{r}_\alpha - \boldsymbol{r}'_\gamma|}dV'_\gamma dV_\alpha\right)\frac{d}{dt}\left(a_\gamma\varepsilon_0(\varepsilon_\gamma - 1)\frac{dE_y}{dt}\right) = \\
&= L_{p\alpha\gamma}\frac{dI_y^P}{dt}
\end{aligned} \tag{90}$$

where the polarization $I_y^P$ current appears. Again, the mutual partial inductance between cells $\alpha$ and $\gamma$ can be evaluated by means of the same formula (89). The same consideration apply to the fifth term.
The last three terms of (85) describe the electric field produced in cell $\alpha$ by the charge located on the surface of cells $\alpha,\ \beta$ and $\delta$. It is to point out that the coefficients of potential describing such couplings are the same as in the free space. Let's consider point $\boldsymbol{r}$ is located in the dielectric cell $\gamma$; equation (77) becomes:

$$\begin{aligned}
E_y(\boldsymbol{r}, t) \quad &+ \quad \frac{\mu}{4\pi}\int_{V'_\alpha} K(\boldsymbol{r}, \boldsymbol{r}')\frac{\partial J_y^C(\boldsymbol{r}', t_d)}{\partial t}dV'_\alpha + \frac{\mu}{4\pi}\int_{V'_\beta} K(\boldsymbol{r}, \boldsymbol{r}')\frac{\partial J_y^C(\boldsymbol{r}', t_d)}{\partial t}dV'_\beta \\
&+ \quad \varepsilon_0(\varepsilon_\gamma - 1)\frac{\mu}{4\pi}\int_{V'_\gamma} K(\boldsymbol{r}, \boldsymbol{r}')\frac{\partial^2 E_y(\boldsymbol{r}', t_d)}{\partial t^2}dV'_\gamma + \\
&+ \quad \varepsilon_0(\varepsilon_\delta - 1)\frac{\mu}{4\pi}\int_{V'_\delta} K(\boldsymbol{r}, \boldsymbol{r}')\frac{\partial^2 E_y(\boldsymbol{r}', t_d)}{\partial t^2}dV'_\delta + \\
&+ \quad \frac{1}{4\pi\varepsilon_0}\int_{S'_\alpha}\frac{\partial K(\boldsymbol{r}, \boldsymbol{r}')}{\partial y}q^T(\boldsymbol{r}', t)dS'_\alpha + \frac{1}{4\pi\varepsilon_0}\int_{S'_\beta}\frac{\partial K(\boldsymbol{r}, \boldsymbol{r}')}{\partial y}q^T(\boldsymbol{r}', t)dS'_\beta + \\
&+ \quad \frac{1}{4\pi\varepsilon_0}\int_{S'_\delta}\frac{\partial K(\boldsymbol{r}, \boldsymbol{r}')}{\partial y}q^T(\boldsymbol{r}', t)dS'_\delta = 0
\end{aligned} \tag{91}$$

The Galerkin's testing procedure is applied leading to find the corresponding equivalent circuits. The integration of the first term in (91) allows to define a voltage drop across a volume dielectric cell:

$$\frac{1}{a_\gamma}\int_{a_\gamma}\int_{l_\gamma} E_y(\boldsymbol{r}, t)dl_\gamma da_\gamma = \frac{1}{a_\gamma}a_\gamma l_\gamma E_y(t) = v_{c_\gamma} \tag{92}$$

A polarization current flows through the dielectric cell $\gamma$:

$$\begin{aligned}
I_y^{POL} \quad &= \quad J_y^{POL}a_\gamma = \left(\varepsilon_0(\varepsilon_\gamma - 1)\frac{dE_\gamma}{dt}\right)a_\gamma = \left(\varepsilon_0(\varepsilon_\gamma - 1)\frac{dE_\gamma}{dt}\right)\frac{l_\gamma}{l_\gamma}a_\gamma = \\
&= \quad \frac{d}{dt}\left[\left(\frac{\varepsilon_0(\varepsilon_\gamma - 1)a_\gamma}{l_\gamma}\right)(l_\gamma E_y)\right] = C_e\frac{dv_{c_\gamma}}{dt}
\end{aligned} \tag{93}$$

where capacitance $C_e$ is named *excess capacitance* and defined as:

$$C_e = \frac{\varepsilon_0(\varepsilon_\gamma - 1)a_\gamma}{l_\gamma} \tag{94}$$

The second and third terms in (91) describe an inductive coupling. The fourth term allows to define the partial self inductance of dielectric cell $\gamma$:

$$\begin{aligned}
&\varepsilon_0(\varepsilon_\gamma - 1)\frac{\mu}{4\pi}\frac{1}{a_\gamma}\int_{V_\gamma}\int_{V'_\gamma} K(\boldsymbol{r}_\gamma, \boldsymbol{r}'_\gamma)\frac{\partial^2 E_y(\boldsymbol{r}_\gamma, t_d)}{\partial t^2}dV'_\gamma dV_\gamma = \\
= \quad &\left(\frac{\mu}{4\pi}\frac{1}{a_\gamma a_\gamma}\int_{V_\gamma}\int_{V'_\gamma} K(\boldsymbol{r}_\gamma, \boldsymbol{r}'_\gamma)dV'_\gamma dV_\gamma\right)\frac{d}{dt}\left(a_\gamma\varepsilon_0(\varepsilon_\gamma - 1)\frac{dE_y}{dt}\right) = \\
= \quad &L_{p\gamma\gamma}\frac{dI_y^{POL}}{dt}
\end{aligned} \tag{95}$$

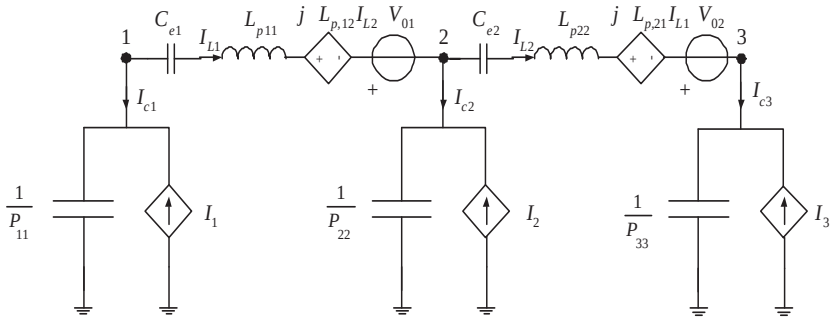


Fig. 11. PEEC equivalent circuit for dielectrics.

The last term allows to evaluate the mutual partial inductance between dielectric cells $\gamma$ e $\delta$:

$$L_{p\gamma\delta} = \frac{\mu}{4\pi a_\gamma a_\delta} \int_{V_\gamma} \int_{V'_\delta} \frac{1}{\boldsymbol{r}_\gamma - \boldsymbol{r}'_\delta} dV'_\delta dV_\gamma \tag{96}$$

Again, the last three terms are analogous to those evaluated in the free space. To summarize, ideal (lossless) dielectrics are modeled by volume cells characterized by the excess capacitance in series to the equivalent circuit for the inductive coupling described in terms of self and partial inductances, computed in free space. Fig. 11 shows the PEEC equivalent circuit of a dielectric bar assuming $N_v = 2$, $N_s = N = 3$. More recently PEEC models of dispersive and lossy dielectrics have been proposed [25]- [27].

### *A. External incident Electric Fields*

When analyzing EMC problems the excitation can be represented by current, voltage-sources and external electric fields as well. The incorporation of incident fields in the PEEC method is detailed in [28] where a source equivalence, $V_0$, is derived from the left hand side in (20a). The equivalent voltage source, $V_0$, is placed in series with each inductive volume cell equivalent circuit and calculated for a volume cell $m$ using

$$V_{0_m}(t) = \frac{1}{a_m} \int_{a_m} \int_{l_m} \boldsymbol{E}^i(\boldsymbol{r}, t) da\ dl \tag{97}$$

where

$$\boldsymbol{E}^i(\boldsymbol{r}, t) = E^i_x(\boldsymbol{r}, t)\hat{x} + E^i_y(\boldsymbol{r}, t)\hat{y} + E^i_z(\boldsymbol{r}, t)\hat{z} \tag{98}$$

## VI. Analysis of PEEC models

The analysis of PEEC models can be carried out in both the frequency and time domain by means of the same circuit.

### *A. Frequency domain solver*

A PEEC frequency domain solver can be obtained just collecting equations (55) and (56) (the dependence on the frequency has been omitted for simplicity):

$$\begin{bmatrix} -\boldsymbol{A} & -(\boldsymbol{R} + j\omega\boldsymbol{L}_p) \\ j\omega\boldsymbol{P}^{-1} & -\boldsymbol{A}^t \end{bmatrix} \cdot \begin{bmatrix} \boldsymbol{\Phi} \\ \boldsymbol{I}_L \end{bmatrix} = \begin{bmatrix} \boldsymbol{V}_0 \\ \boldsymbol{I}_s \end{bmatrix} \tag{99}$$

*1) Solution of dense linear systems:* An efficient and accurate solution of the linear system (99) is extremely important for the performance of the PEEC solver. The most common technique to solve linear systems is the LU decomposition [29]. Although elegant such method is not practical for solving large and dense linear systems as its complexity is $O(n^3)$, being $n$ the number of the unknowns. It is much more convenient to use Krylov subspace iterative methods [29]. Many different implementation variants are available; the most popular is GMRES [30] whose complexity is $O(n^2)$ as requires matrix-vector products and converges in a very small number of iterations if an efficient *pre-conditioner* is used. Furthermore, the matrix-vector product can be accelerated by using fast-multipole techniques [31]–[34] or precorrected-FFT methods [35] which may reduce the complexity to $O(n \log(n))$.

*B. Time domain solver*

The development of time domain PEEC solver needs to consider the delay in the coupling terms. In the following we assume that partial inductances and coefficients of potential are evaluated as static coefficients, thus assuming a center to center approximation (60) and (68).

The coupling inductance $Lp_{mn}$ between the partial inductances $Lp_{mm}$ and $Lp_{nn}$ leads to the neutral delay term which is related to the physical spacing of the inductive cells $m$ and $n$ as given by

$$t'_{mn} = t - \frac{|\boldsymbol{r}_m - \boldsymbol{r}_n|}{c} = t - \tau \tag{100}$$

Hence, the coupled inductive voltage takes the form:

$$v_{mn} = Lp_{mn} \frac{di_n(t'_{mn})}{dt}, \tag{101}$$

Analogously, the capacitive coupling with delays needs to be implemented. The general form of the capacitive term is $\boldsymbol{\Phi}(\omega) = \boldsymbol{PQ}(\omega)$ where $\boldsymbol{P}(\omega)$ is the coefficient of potential matrix. The corresponding time domain implementation can be derived from (50):

$$i_{ck}(t) = \frac{1}{P_{kk}} \frac{\partial \Phi_k}{\partial t} - \sum_{\substack{m=1 \\ m \neq k}}^{N_s} \frac{P_{km}}{P_{kk}} i_{cm}(t'_{km}) \tag{102}$$

where $i_{ck}$ is the total capacitive current for cell $k$. We may assign more than one delay for each cell pair leading to potentially multiple distances $R_{km}$ between points on two cells $k$ and $m$.

The above formulation for a linear PEEC circuit consisting of PEEC models, using the Modified Nodal Analysis (MNA) technique [36], can be written as the following NDDE

$$\boldsymbol{C_0}\, \dot{\boldsymbol{x}} + \boldsymbol{G_0 x} = \sum_i \boldsymbol{G_i}\, \boldsymbol{x}(t - \tau_i) + \sum_i \boldsymbol{C_i}\, \dot{\boldsymbol{x}}(t - \tau_i) + \sum_i \boldsymbol{B u_i}(t - \tau_i) \tag{103}$$

where $\boldsymbol{C_0}$ and $\boldsymbol{G_0}$ represent the time dependent and the static portion of the non-delayed part, respectively, while $\boldsymbol{C_i}$ and $\boldsymbol{G_i}$ correspond to the elements with a delay $\tau_i$. Finally, $\boldsymbol{B}$ is the input selector matrix and $\boldsymbol{u}$ are the inputs or forcing voltages and currents. The size of this combined electromagnetic and circuit (EM/Ckt) problem can be extremely large where the $\boldsymbol{L}_p$ and $\boldsymbol{P}$ coupling coefficients matrices are dense and very large. However, as is evident from (103), the solution of the left hand part is importantly very sparse since it contains only the non-retarded part or the slightly retarded part of the matrix, depending on the time step $h$. In a time domain solver, the couplings have to be computed by picking up values in the past, delayed by the appropriate $\tau$ for the time domain from stored waveforms. Hence, the couplings are already known and the values are stamped into the known right hand side of the system rather than the MNA circuit coefficient matrix. The basic solution complexity is $O(n^2)$ where $n$ is the system size.

One of the most important aspects which at present reduces the generality of the time domain approach is the long time stability of the solution. Improvements to the stability have been made over thirty years by numerous researchers. In [37], the general stability issue with full-wave time domain integral equation solution is described. Since then, much more progress has been made on the stability issue. For example. the impact of the delay points on the conductors was studied in [38] and the introduction of further delay points or cell subdivisions of the conductors on the stability issue was considered for PEEC models in [39]. A refinement strategy for the delay assignment is presented in [40]. More recently the stability of quasi-static PEEC models has been investigated [41].

The choice of the numerical integration method is very important for several aspects of the solution. Early work on the solution of time domain electromagnetic integral equation solvers used explicit methods [37]. However, it became clear that explicit forward Euler type methods could only lead to stable solutions for very special cases and for extremely small time steps. For this reason, several researchers started to employ implicit methods for the time domain PEEC methods which are especially suited for this type of problem, *e.g.*, [42], [43]. One of the key considerations for the choice of the method is the behavior of the stability function $R(z)$ where $z = \lambda h$ where $\lambda$ is the eigenvalue and $h$ is the time step [44]. We clearly require that the stability functions which decay with $z \to \infty$. This is evident from the last section since, preferably, we

do have several mechanisms in our model to dampen the amplitude above $f_M$ such that a strong feedback reduction occurs without impacting the solution behavior below $f_M$. Three methods which are well suited for the task are the backward Euler method, the $\theta$ method for $\theta > 0.5$, and the Lobatto III-C method. In fact, the Lobatto III-C method decays as $1/(z^2)$, which is very desirable. However, as shown below, the size of the system matrix is a factor 2 larger than for the $\theta$ or the BE methods. The frequently used trapezoidal rule was shown to be one of the worst methods for these systems [43]. The stability function of the BE formula decays asymptotically as $1/(z)$, which is also very desirable. NDDE equations can be solved by an adaptation of the RK methods for ODEs, *e.g.*, [45].

Finally, it is also to be pointed out that the solution of (103) can be accelerated by means of the fast multipole method and multi-function techniques [46]- [47].

## VII. Examples

### A. Crosstalk problem

An 8 lead tape automated bonding (TAB) interconnect has been modeled. Figure 12 shows the geometry of the TAB. It is $l = 350$ mil long, conductor width and separation are $w = 4$ mil , $S = 8$ mil at inner side, $w = 8$ mil, $S = 16$ mil at outer side, respectively. The line 3 from the bottom is driven by a unit voltage step. The input and output port voltages $V_{in}$ and $V_{out}$ of the driven line are shown in Fig. 13 along with the near and far end voltages induced on the line 4.

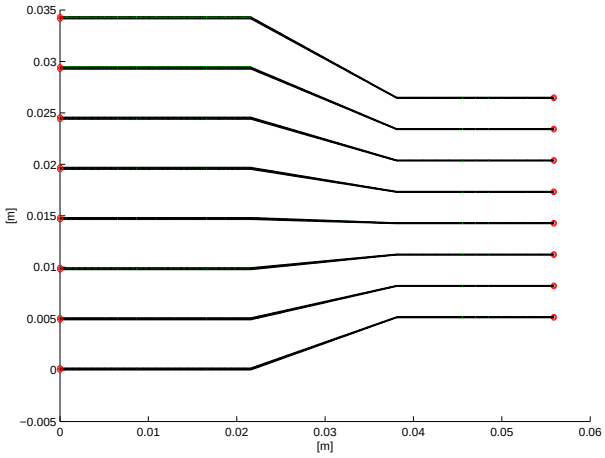


Fig. 12. Crosstalk analysis.

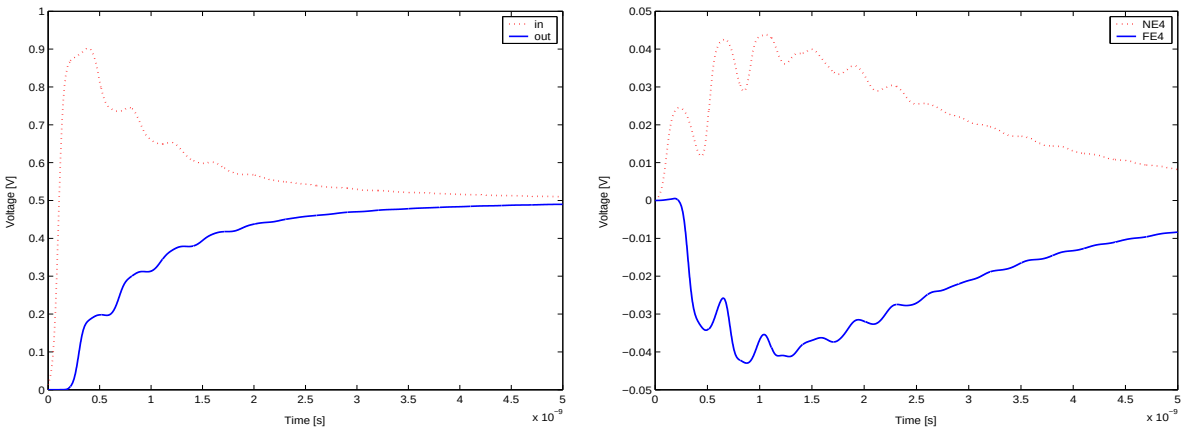


Fig. 13. Crosstalk analysis voltages. Driven line (3): $V_{in}$, $V_{out}$; victim-line (4): $V_{NE}$, $V_{FE}$.

*B. Signal integrity problem*

The second example considers the propagation of a signal on a microstrip structure on a dielectric substrate. Its geometry is shown in Fig. 14.

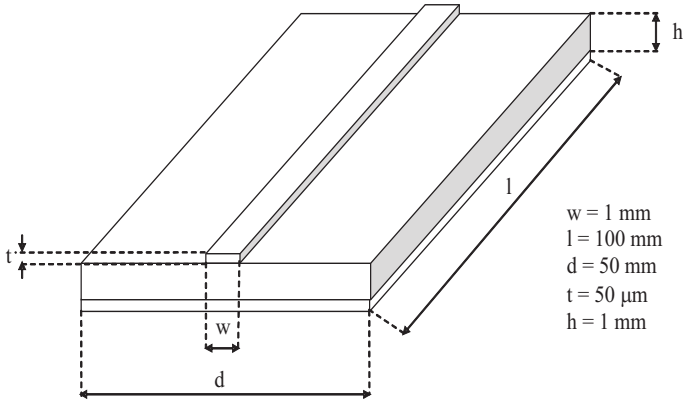


Fig. 14. Microstrip line.

The dielectric permittivity is $\varepsilon_3.4\varepsilon_0$. The microstrip transmission line is excited by 7 ns pulse with 2 ns rise and fall time (see Fig. 15). The terminations are loaded by 50 Ω resistances. Polarization currents are introduced to take into account the presence of inhomogeneous dielectric volumes. As a consequence of this the free-space Green's function is used in computing PEEC coupling parameters. All the conductive and dielectric volume are discretized by means of hexahedral elements according to the general approach presented in [23]. The surfaces are covered by quadrilateral elements where free and/or bound charge is localized. The analysis has been carried out using two different spatial discretization with an increasing number of current and potential basis functions. For both the cases PEEC parameters have been evaluated using a numerical routine implementing the Gauss-Legendre algorithm (GL) and the Fast Multipole Method [34]. Fig. 16 shows the voltage waveforms at the input and output ports as obtained by means of the two aforementioned techniques. They are almost perfectly overlapped.

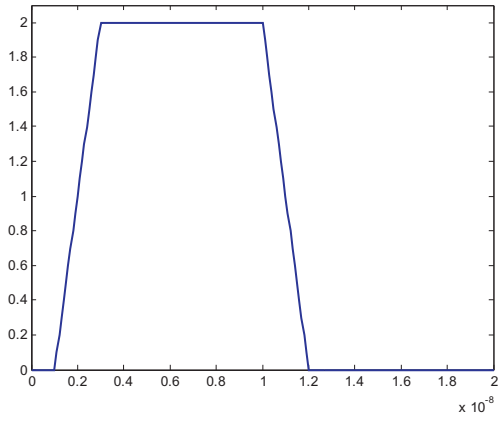


Fig. 15. Microstrip line excitation.

*C. Direct lightning stroke*

In the third case study the direct lightning stroke of a large structure is considered. It is constituted by a 100 m long semi-cylindrical covering grounded every 15 m. Fig. 17 shows the configuration under analysis.

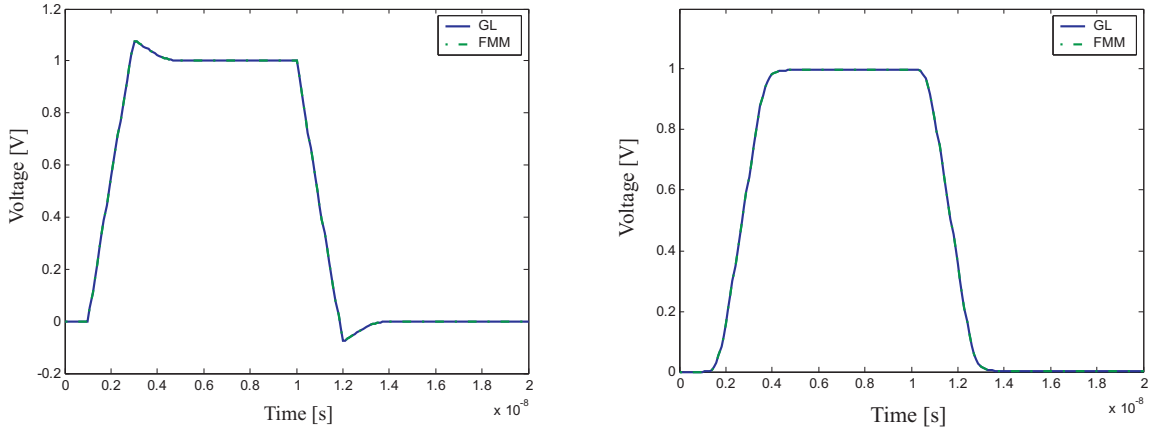


Fig. 16. Microstrip voltages at the input (left) and output (right) ports.

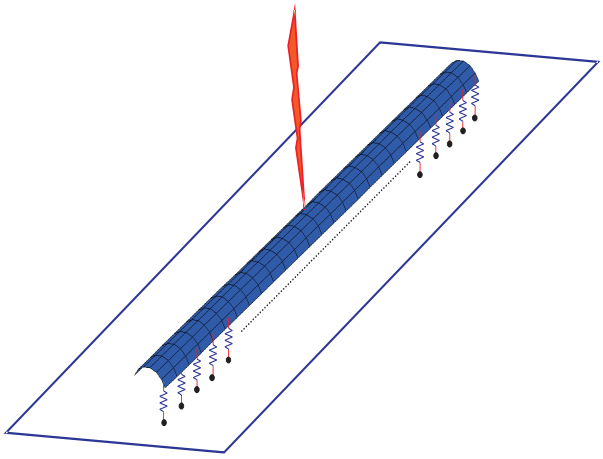

Fig. 17. Direct lightning stroke of a long structure.

The overall structures has been discretized with 2500 patches - 12000 spatial basis functions considering both currents and potentials to infinity. A direct stroke hits the covering just in the middle; thus, currents flow and far end voltages arise. Potential at the striking point and far ends are shown in Fig. 18.

### *D. Parasitic effects in a buck-boost electronic converter*

One of the main advantage of the PEEC method is relies in the easy incorporation of linear and non linear lumped elements. In the last case study a buck-boost converter has been modeled. Its aim is to convert the DC voltage $V_d$ to the voltage $V_{load}$. The equivalent circuit of the buck-boost converter is shown in Fig. 19. The nominal values of the parameters are: $V_d = 8.5$ V, $L = 10$ mH, $C = 100$ mF, $R_{load} = 8$ $\Omega$, switching frequency $f_s = 100$ kHz, switch duty ratio $0.75$. The thickness of the copper conductors constituting the interconnect is assumed to be 18 mm. Due to the quite high frequency content of currents flowing in the interconnect, inductive effects need to be considered. The overall structure has been discretized in 288 capacitive cells with 127 different electrical nodes and 288 inductive cells; thus the zero thickness approximation has been assumed. The parasitic effects of the interconnect (in Fig. 20) cause the output voltage to be affected by a significant ripple as shown in Fig. 21.

## VIII. Conclusions

This tutorial paper presented a review of the Partial Element Equivalent Circuit (PEEC) method. Starting from the volume integral formulation of Maxwell's equation, the derivation of the technique has been

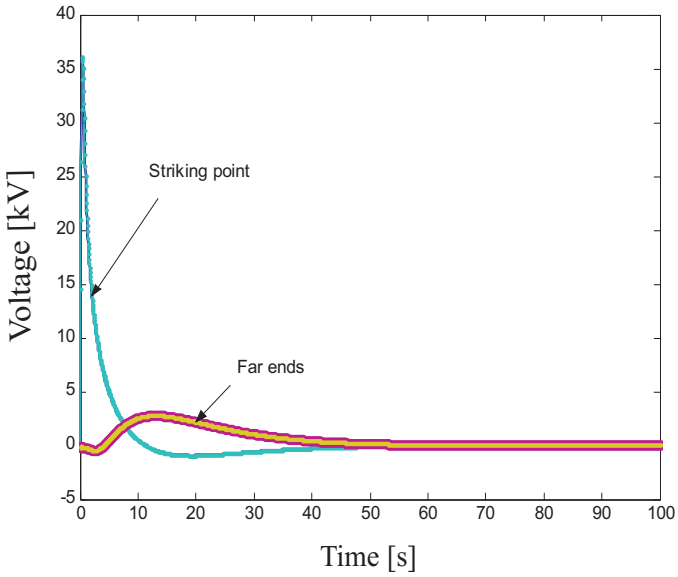


Fig. 18. Potential at the striking point and far ends.

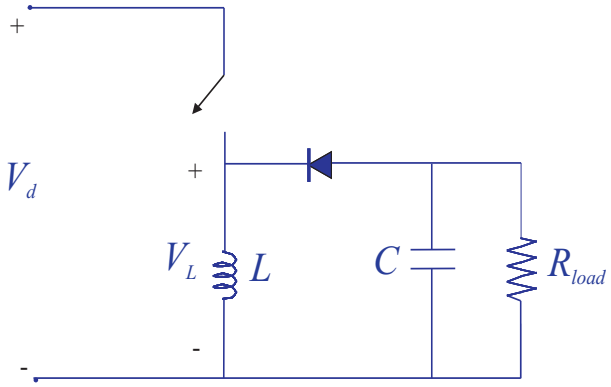


Fig. 19. Buck-boost converter.

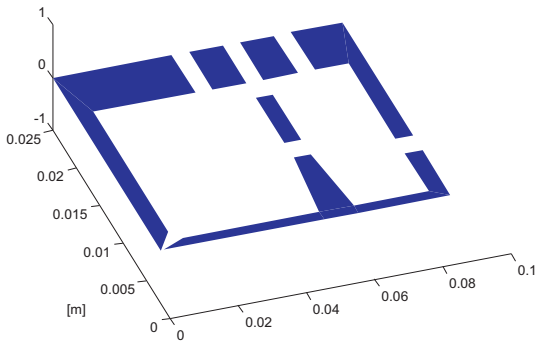


Fig. 20. Buck-boost converter interconnect.

described step-by-step with the aim to help the reader to develop his own PEEC solver focusing on the

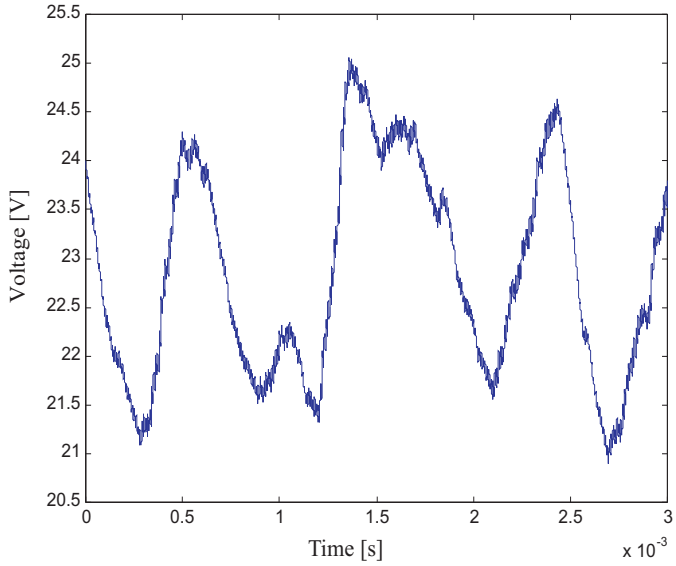


Fig. 21. Buck-boost converter output voltage.

different aspects of its implementation. It has been pointed out that the PEEC method is very well suited to be adopted to analyze mixed electromagnetic and circuit problems like those arising in EMC, EMI and SI areas, as the presented examples have shown.

## REFERENCES


[1] J. M. Jin. *The Finite Element Method in Electromagnetics*. John Wiley and Sons, New York, 2nd edition, 2002.

[2] K. S. Yee. Numerical Solution of Initial Boundary Value Problems Involving Maxwell's Equations in Isotropic media. *IEEE Transactions on Antennas and Propagation*, 14(5):302–307, May 1966.

[3] A. Taflove. *Advances in Computational Electrodynamics*. Artech House, 1998.

[4] A. Taflove and S. C. Hagness. *Computational Electrodynamics*. Artech House, 2000.

[5] R. F. Harrington. *Field Computation by Moment Methods*. Macmillan, New York, 1968.

[6] A. E. Ruehli. Equivalent Circuit Models for Three Dimensional Multiconductor Systems. *IEEE Transactions on Microwave Theory and Techniques*, MTT-22(3):216–221, March 1974.

[7] A. E. Ruehli. Survey of computer-aided electrical analysis of integrated circuit interconnections. *IBM Journal of Research and Development*, 23(6):626–639, November 1979.

[8] H. Heeb and A. Ruehli. Three-Dimensional Interconnect Analysis Using Partial Element Equivalent Circuits. *IEEE Transactions on Circuits and Systems*, 38(11):974–981, November 1992.

[9] C. A. Balanis. *Advanced Engineering Electromagnetics*. John Wiley and Sons, New York, 1989.

[10] L. W. Nagel. SPICE: A computer program to simulate semiconductor circuits. Electr. Res. Lab. Report ERL M520, University of California, Berkeley, May 1975.

[11] N. Morita, N. Kumagai, J. R. Mautz. *Integral Equation Methods for Electromagnetics*. Artech House, 1990.

[12] A. W. Glisson and D. R. Wilson. Simple and efficient numerical methods for problems of electromagnetic radiation and scattering from surfaces. *IEEE Transactions on Antennas and Propagation*, 28:593–603, 1980.

[13] S. M. Rao, D.R. Wilton, and A.W. Glisson. Electromagnetic scattering by surfaces of arbitrary shape. *IEEE Transactions on Antennas and Propagation*, 30:409–418, May 1982.

[14] S. M. Rao and D. R. Wilton. Transient scattering by conducting surfaces of arbitrary shape. *IEEE Transactions on Antennas and Propagation*, 39(1):56–61, 1991.

[15] J. J. H. Wang. *Generalized Moment Method in Electromagnetics*. John Wiley and Sons, New York, 1991.

[16] B. M. Kolundzija and B. D. Popovic. Entire-domain Galerkin method for analysis of metallic antennas and scatterers. *Proceedings of the IEE H*, 140(1):1–10, January 1993.

[17] A. E. Ruehli. Inductance Calculations in a Complex Integrated Circuit Environment. *IBM Journal of Research and Development*, 16(5):470–481, September 1972.

[18] F. W. Grover. *Inductance calculations: Working formulas and tables*. Dover, 1962.

[19] P. A. Brennan, N. Raver and A. E. Ruehli. Three-Dimensional Inductance Computations with Partial Element Equivalent Circuits. *IBM Journal of Research and Development*, 23(6):661–668, November 1979.

[20] A. E. Ruehli, P. A. Brennan. Efficient Capacitance Calculations for Three-Dimensional Multiconductor Systems. *IEEE Transactions on Microwave Theory and Techniques*, 21(2):76–82, February 1973.

[21] P. A. Brennan, A. E. Ruehli. Capacitance Models for Integrated Circuit Metallization Wires. *IEEE Transactions on Solid State Circuits*, 10(6):530–536, December 1975.
[22] G. Antonini, A. Orlandi, A. Ruehli. Analytical Integration of Quasi-Static Potential Integrals on Non-Orthogonal Coplanar Quadrilaterals for the PEEC Method. *IEEE Transactions on Electromagnetic Compatibility*, 44(2):399–403, May 2002.
[23] A.E. Ruehli, G. Antonini, J. Esch, J. Ekman, A. Mayo, A. Orlandi. Non-Orthogonal PEEC Formulation for Time and Frequency Domain EM and Circuit Modeling. *IEEE Transactions on Electromagnetic Compatibility*, 45(2):167–176, May 2003.
[24] A. E. Ruehli and H. Heeb. Circuit Models for Three-Dimensional Geometries Including Dielectrics. *IEEE Transactions on Microwave Theory and Techniques*, 40(7):1507–1516, July 1992.
[25] G. Antonini. PEEC Modelling of Debye Dispersive Dielectrics. In *Electrical Engineering and Electromagnetics*, pages 126–133. WIT Press, C. A. Brebbia, D. Polyak Editors, 2003.
[26] G. Antonini, A. E. Ruehli, A. Haridass. Including Dispersive Dielectrics in PEEC Models. In *Digest of Electr. Perf. Electronic Packaging*, Princeton, NJ, USA, October 2003.
[27] G. Antonini, A. E. Ruehli, A. Haridass. PEEC Equivalent Circuits for Dispersive Dielectrics. In *Proceedings of Piers-Progress in Electromagnetics Research Symposium*, Pisa, Italy, March 2004.
[28] A. E. Ruehli, J. Garrett, C. R. Paul. Circuit models for 3d structures with incident fields. In *Proc. of the IEEE Int. Symp. on Electromagnetic Compatibility*, pages 28–31, Dallas, Tx, August 1993.
[29] A. Quarteroni. *Numerical Mathematics*. Springer-Verlag, 2000.
[30] Y. Saad, M. Schultz. GMRES: A Generalized Minimal Residual Algorithm for Solving Nonsymmetric Linear Systems. *Siam J. Scientific and Statistical Computing*, 7(3):856–869, 1986.
[31] N. Engheta, W. D. Murphy, V. Rokhlin, M. S. Vassilou. The fast multipole method (FMM). In *PIERS*, July 1991.
[32] R. Coifman, V. Rokhlin and S. Wandzura. The fast multipole method: A pedestrian description. *IEEE Antenna and Propagation Magazine*, 35(3):7–12, 1993.
[33] J M. Song and W. C. Chew. Multilevel fast-multipole algorithm for solving combined field integral equations of electromagnetic scattering. *Microwave and Optical Technology Letters*, 10, 1995.
[34] G. Antonini, A. E. Ruehli. Fast Multipole and Multi-Function PEEC Methods. *IEEE Transactions on Mobile Computing*, 2(4):288–298, October-December 2003.
[35] J. R. Phillips and J. K. White. A Precorrected-FFT Method for Electrostatic Analysis of Complicated 3-D Structures. *IEEE Transactions on Computer-Aided Design of Integrated Circuits and Systems*, 16(10):1059–1072, October 1997.
[36] C. Ho, A. Ruehli, P. Brennan. The Modified Nodal Approach to Network Analysis. *IEEE Transactions on Circuits and Systems*, pages 504–509, June 1975.
[37] B.P. Rynne. Comments on a stable procedure in calculating the transient scattering by conducting surfaces of arbitary shape. *IEEE Transactions on Antennas and Propagation*, APP-41(4):517–520, April 1993.
[38] A. E. Ruehli, U. Miekkala, and H. Heeb. Stability of Discretized Partial Element Equivalent EFIE Circuit Models. *IEEE Transactions on Antennas and Propagation*, 43(6):553–559, June 1995.
[39] J. Garrett, A.E. Ruehli, and C.R. Paul. Accuracy and stability improvements of integral equation models using the partial element equivalent circuit PEEC approach. *IEEE Transactions on Antennas and Propagation*, 46(12):1824–1831, December 1998.
[40] J. Pingenot, S. Chakraborty, V. Jandhyala. Polar integration for exact space-time quadrature in time-domain integral equations. (submitted for publication). *IEEE Transactions on Antennas and Propagation*, 2006.
[41] J. Ekman, G. Antonini, A. Orlandi and A. E. Ruehli. The Impact of Partial Element Accuracy for PEEC Model Stability. *IEEE Transactions on Electromagnetic Compatibility*, 48(1), February 2006.
[42] A. E. Ruehli, U. Miekkala, A. Bellen, and H. Heeb. Stable time domain solutions for EMC problems using PEEC circuit models. In *Proc. of the IEEE Int. Symp. on Electromagnetic Compatibility*, Chicage,Ill, August 1994.
[43] A. Bellen, N. Guglielmi, A. Ruehli. Methods for Linear Systems of Circuit Delay Differential Equations of Neutral Type. *IEEE Transactions on Circuits and Systems*, 46:212–216, January 1999.
[44] E. Hairer and G. Wanner. *Solving ordinary differential equations II, Stiff and differential algebraic problems*. Springer-Verlag, New York, 1991.
[45] A. Bellen, M. Zennaro. Strong contractivity properties of numerical methods for ordinary delay differential equations. *Applied Numer. Math.*, 9:321–346, 1992.
[46] G. Antonini. Fast Multipole Formulation for PEEC Frequency Domain Modeling. *Applied Computatational Electromagnetic Society Newsletter*, 17(3), November 2002.
[47] G. Antonini. Fast Multipole Method for Time Domain PEEC Analysis. *IEEE Transactions on Mobile Computing*, 2(4):275–287, October-December 2003.